

**UNIVERSIDADE FEDERAL DE PELOTAS**

**Centro de Ciências Químicas, Farmacêuticas e de Alimentos**

**Programa de Pós-Graduação em Bioquímica e Bioprospecção**



**TESE DE DOUTORADO**

**Síntese e atividade antiglioblastoma *in vitro* e *in vivo* de 2,4-tiazolidinedionas**

**Alana de Vasconcelos**

**Pelotas, 2020**

Universidade Federal de Pelotas / Sistema de Bibliotecas  
Catalogação na Publicação

V331s Vasconcelos, Alana de

Síntese e atividade antiglioblastoma *in vitro* e *in vivo* de 2,4-tiazolidinedionas / Alana de Vasconcelos ; Wilson João Cunico Filho, orientador ; Francieli Moro Stefanello, coorientadora. — Pelotas, 2020.

92 f. : il.

Tese (Doutorado) — Programa de Pós-Graduação Bioquímica e Bioprospecção, Centro de Ciências Químicas Farmacêuticas e de Alimentos, Universidade Federal de Pelotas, 2020.

1. 2,4-tiazolidinediona. 2. Antiglioma. 3. Antitumoral. 4. Reação one-pot. 5. N-alquilação. I. Cunico Filho, Wilson João, orient. II. Stefanello, Francieli Moro, coorient. III. Título.

CDD : 540

**Alana de Vasconcelos**

**Síntese e atividade antiglioblastoma *in vitro* e *in vivo* de 2,4-tiazolidinedionas**

Tese apresentada ao Programa de Pós-Graduação em Bioquímica e Bioprospecção da Universidade Federal de Pelotas, como requisito parcial à obtenção do título de Doutora em Ciências (Bioquímica e Bioprospecção).

Orientador: Prof. Dr. Wilson Cunico

Co-orientadora: Prof<sup>a</sup>. Dr<sup>a</sup>. Francieli Moro Stefanello

Pelotas, 2020

**Alana de Vasconcelos**

**Síntese e atividade antiglioblastoma *in vitro* e *in vivo* de 2,4-tiazolidinedionas**

Tese apresentada, como requisito parcial, para obtenção do grau de Doutora em Ciências, Programa de Pós-graduação em Bioquímica e Bioprospecção, Centro de Ciências Químicas, Farmacêuticas e de Alimentos, Universidade Federal de Pelotas.

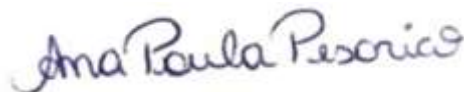
Data da defesa: 29/05/2020 às 14 h

Banca Examinadora:



---

Prof. Dr. Wilson Cunico (Orientador) - Doutor em Química pela Universidade Federal de Santa Maria.



---

Prof<sup>a</sup>. Dr<sup>a</sup>. Ana Paula Pesarico - Doutora em Ciências Biológicas (Bioquímica Toxicológica) pela Universidade Federal de Santa Maria.



---

Prof. Dr. Geonir Machado Siqueira - Doutor em Química pela Universidade Federal de Santa Maria.



---

Prof. Dr. Patrick Teixeira Campos - Doutor em Química pela Universidade Federal de Santa Maria.

A todos que por um motivo ou outro me ajudaram a adquirir este título, em especial ao meu Orientador Wilson Cunico, ao meu Pai Alceu Dip de Vasconcelos e a minha Mãe Rossana Maria de Vasconcelos.

## **AGRADECIMENTOS**

Agradeço a todas as pessoas que contribuíram diretamente ou indiretamente para a realização deste trabalho, em especial:

- Ao professor Dr. Wilson Cunico pela grande ajuda e orientação durante o doutorado.
- A professora Dr<sup>a</sup>. Francieli Moro Stefanello pela co-orientação e colaboração.
- Ao professor Geonir Machado Siqueira pela ajuda.
- Aos alunos de iniciação científica Ana Júlia Zulian e Larissa Moura pela ajuda.
- As alunas e professores (as), Nathalia Stark Pedra, Natália Pontes Bona, Mayara Sandrielly Pereira Soares, Luiza Spohr, Roselia Maria Spanevello, Alethaea Gatto Barschak e Rodrigo de Almeida Vaucher, de outros grupos de pesquisa, pela colaboração com o estudo.
- A banca examinadora.
- Aos colegas do laboratório LaQuiABio Adriana Neves, Bruna Bento, Bruna Moreira e José Coan pela colaboração.
- As entidades financiadoras CAPES e FAPERGS.

*“Há duas formas para viver a sua vida. Uma é acreditar que não existe milagre. A outra é acreditar que todas as coisas são um milagre.”*

*Albert Einstein*

## RESUMO

VASCONCELOS, Alana. **Síntese e atividade antiglioblastoma *in vitro* e *in vivo* de 2,4-tiazolidinedionas**, 2020. Programa de Pós-Graduação em Bioquímica e Bioprospecção, Universidade Federal de Pelotas, Pelotas, 2020.

As tiazolidinedionas (TZDs) representam uma classe importante de compostos heterocíclicos que possuem atividades biológicas versáteis, incluindo ação anticâncer. No presente estudo, dezessete 2,4-tiazolidinedionas foram sintetizadas, identificadas, caracterizadas e analisadas quanto à atividade antiglioblastoma. A síntese dos compostos foi realizada através de reações de Knoevenagel e de *N*-alquilação em uma metodologia *one-pot* utilizando um aparelho de micro-ondas próprio para laboratório em 40 minutos. As estruturas químicas foram identificadas e caracterizadas por cromatografia gasosa acoplada a espectrômetro de massas (CG-EM) e por ressonância magnética nuclear de hidrogênio e carbono (RMN de  $^1\text{H}$  e  $^{13}\text{C}$ ). A atividade antiglioma foi avaliada *in vitro* pelo ensaio colorimétrico do MTT e após, foi realizado um estudo *in vivo* por meio da implantação intracerebroventricular de células C6 de glioblastoma em ratos Wistar. Os parâmetros comportamentais (teste de reconhecimento de objetos e campo aberto) e bioquímicos séricos foram determinados no modelo pré-clínico. Todos os compostos sintetizados reduziram a viabilidade celular em linhagem celular de glioblastoma de ratos C6 e quinze compostos foram citotóxicos em linhagem de camundongos GL261. Nenhum dos compostos demonstrou toxicidade em cultura primária de astrócitos, evidenciando assim seletividade para as células tumorais. Os compostos **4Cl**  $\text{IC}_{50} = 28,51 \mu\text{M}$  e **4DI**  $\text{IC}_{50} = 54,26 \mu\text{M}$ , ambos com  $\text{R}^2 = 4\text{-F}$ , apresentaram os melhores resultados, supõem-se, portanto, que o átomo de flúor na posição quatro do anel B seja importante para a atividade antiglioblastoma. O composto **4Cl**, com o menor  $\text{IC}_{50}$ , foi selecionado para a análise *in vivo*, na qual se constatou que o tratamento por 15 dias com a dose de 10 mg/kg administrada pela via intragástrica foi capaz de reduzir qualitativamente o volume tumoral e normalizar os níveis glicêmicos. Não houve alteração no perfil lipídico e conteúdo proteico, assim como não ocorreram modificações nos marcadores bioquímicos de dano renal após o tratamento. Os níveis da aspartato aminotransferase não foram alterados em nenhum dos grupos experimentais, entretanto foi verificado um aumento da alanina aminotransferase, ambas as enzimas utilizadas para avaliar dano hepático. O composto **4Cl** reverteu a hipolocomoção encontrada nos animais não tratados, bem como a redução do ganho de peso induzida pelo glioblastoma. De acordo com os resultados obtidos nos testes *in vitro*, todos os compostos foram promissores para a atividade antiglioblastoma, principalmente o **4Cl**, que obteve a maior redução da viabilidade de células C6 e também baixa toxicidade em cultivo de astrócitos. O **4Cl** também demonstrou atividade antiglioblastoma *in vivo*, sendo assim um potencial candidato para estudos pré-clínicos em outros modelos animais.

Palavras-Chave: 2,4-tiazolidinediona; Antiglioma, Antitumoral; Reação *one-pot*; *N*-alquilação e Knoevenagel.

## ABSTRACT

VASCONCELOS, Alana. **Synthesis and *in vitro* and *in vivo* anti-glioblastoma activity of 2,4-thiazolidinediones**, 2020. Doctoral thesis, Graduate Program in Biochemistry and Bioprospecting, Federal University of Pelotas, Pelotas, 2020.

Thiazolidinediones (TZDs) are an important class of heterocyclic compounds that have versatile biological activities, including anticancer action. In the present study, seventeen 2,4-thiazolidinediones were synthesized, identified, characterized and analyzed for anti-glioblastoma activity. The synthesis of the compounds was performed through Knoevenagel and *N*-alkylation reactions in a one-pot methodology using a microwave oven suitable for the laboratory in 40 minutes. The chemical structures were identified and characterized by gas chromatography coupled to mass spectrometer (GC-MS) and by nuclear magnetic resonance of hydrogen and carbon ( $^1\text{H}$  and  $^{13}\text{C}$  NMR). The anti-glioma activity was evaluated *in vitro* by the MTT colorimetric assay and afterwards, an *in vivo* study was carried out by intracerebroventricular implantation of glioblastoma C6 cells in Wistar rats. The behavioral (object recognition and open field tasks) and serum biochemical parameters were determined in the preclinical model. All the synthesized compounds reduced cell viability in the C6 glioblastoma cell line and fifteen compounds were cytotoxic in the GL261 mouse line. None of the compounds showed toxicity in primary astrocyte culture, thus showing selectivity for tumor cells. The compounds **4CI**  $\text{IC}_{50} = 28.51 \mu\text{M}$  and **4DI**  $\text{IC}_{50} = 54.26 \mu\text{M}$ , both with  $\text{R}^2 = 4\text{-F}$ , showed the best results, therefore, it was assumed that the fluorine atom in position four of ring B is important for anti-glioblastoma activity. Compound **4CI**, with the lowest  $\text{IC}_{50}$ , was selected for the *in vivo* analysis, in which it was found that the treatment for 15 days with the dose of 10 mg/kg administered by intragastric route was able to qualitatively reduce the tumor volume and normalize the glycemic levels. There was no change in the serum lipid profile and protein content, as well as no changes in the biochemical markers of renal damage. As regards liver damage markers, it was observed that aspartate aminotransferase levels were not altered in any of the experimental groups; however, an increase was detected in alanine aminotransferase caused by treatment. The **4CI** compound reverted the hypolocomotion found in untreated animals, as well as the reduction in weight gain induced by glioblastoma. According to the results obtained in the *in vitro* tests, all compounds were promising for anti-glioblastoma activity, mainly **4CI**, which obtained the greatest reduction in the viability of C6 cells and also low toxicity in astrocyte culture. **4CI** also demonstrated anti-glioblastoma activity *in vivo*, thus being a potential candidate for preclinical studies in other animal models.

Key words: 2,4-thiazolidinedione; Anti-glioma; Antitumoral; One-pot reaction; *N*-alkylation and Knoevenagel.

## LISTA DE FIGURAS

<b>Figura 1</b>	Critérios para classificação de gliomas.	22
<b>Figura 2</b>	Mutação da IDH e sua relação com o ciclo do ácido tricarboxílico e vias que levam à tumorigênese após a mutação.	23
<b>Figura 3</b>	Inibição da enzima TET	24
<b>Figura 4</b>	Metiltransferases de DNA (DNMTs) catalisando a transferência do grupo metil para a 5' citosina e desmetilação de 5mC pela enzima TET.	25
<b>Figura 5</b>	Alterações aberrantes da metilação do DNA em locais genômicos específicos em células tumorais.	26
<b>Figura 6</b>	A) Desmetilação do DNA causada pela enzima MGMT e resistência à TMZ.  B) Metilação do promotor do gene da enzima MGMT contribuindo para a ação da TMZ.	27
<b>Figura 7</b>	A) Mecanismo de ação dos fármacos EGFR TKI e depatuxizumabe mafodotin.  B) Mecanismo de ação dos fármacos bevacizumabe e cediranibe.	29
<b>Figura 8</b>	Ativação de genes via PPAR $\gamma$ .	31
<b>Figura 9</b>	A) Trocador Xc e captação de glutamato extracelular através do EAAT2.  B) Redução da expressão do EAAT2 e consequente aumento de glutamato extracelular e suas implicações.	32
<b>Figura 10</b>	Estrutura da 2,4-tiazolidinediona e posições de funcionalização.	34

**Figura 11** A) Estrutura química da cigitazona. 35

B) Estrutura química da pioglitazona.

**Figura 12** TZDs avaliadas no estudo de RÊGO et al. 2014. 37

## LISTA DE ESQUEMA

**Esquema 1** Rota sintética para a obtenção das TZDs. 19

**Esquema 2** Síntese de 3-benzil-5-benzilidenotiazolidina-2,4-diona de maneira *one-pot* em micro-ondas (RADI, et al. 2010). 36

**Esquema 3** Síntese de uma série de TZDs realizada em três etapas pelo método de aquecimento térmico convencional 36

OBS: As demais figuras e tabelas, bem como os esquemas desta tese fazem parte do artigo e/ou do manuscrito e, portanto, não estão elencadas nestas listas.

## LISTA DE ABREVIATURAS E SIGLAS

$^{13}\text{C}$ -NMR	<i>Nuclear magnetic resonance of carbon</i>
2-HG	Ácido 2-hidroxipentérico
5hmC	5-hidroximetilcitosina
5mC	5-metilcitosina
$^1\text{H}$ -NMR	Ressonância magnética nuclear de hidrogênio (em inglês: <i>nuclear magnetic resonance of hydrogen</i> )
ALT	Alanina aminotransferase (em inglês: <i>alanine aminotransferase</i> )
AST	Aspartato aminotransferase (em inglês: <i>aspartate aminotransferase</i> )
CG-EM	Cromatografia gasosa acoplada a espectrômetro de massas
CpG	Citosina-fosfato-guanina
DMF	Dimetilformamida (em inglês: <i>dimethylformamide</i> )
DNMTs	Metiltransferases de DNA (em inglês: <i>DNA methyltransferase</i> )
EAAT2	Transportador excitatório de aminoácidos 2 (em inglês: <i>excitatory amino acid transporter 2</i> )
EGFR	Receptor do fator de crescimento epidérmico
EROs	Espécies reativas de oxigênio
G-CIMP	Fenótipo metilador da ilha de citosina-fosfato-guanina
GC-MS	Cromatografia gasosa acoplada a espectrômetro de massas (em inglês: <i>gas chromatography coupled to mass spectrometer</i> )
HIF-1	Fator induzível por hipoxia 1
IDH	Isocitrato desidrogenase

IGF-1	Fator de crescimento semelhante à insulina (em inglês: <i>insulin-like growth factor</i> )
IGF-1R	Receptor do fator de crescimento semelhante à insulina (em inglês: <i>insulin-like growth factor receptor</i> )
IR	Receptor de insulina (em inglês: <i>insulin receptor</i> )
LPSF / SF-13	(5Z) -5- (3-bromo-benzilideno) -3- (4-nitrobenzil) -tiazolidina- 2,4-diona
MGMT	O6-metilguanina-DNA metiltransferase
MTT	Brometo de 3- (4,5-dimetil) -2,5-difeniltetrazólio (em inglês: <i>3-(4,5-dimethyl)-2,5-diphenyltetrazolium bromide</i> )
P53	Proteína de tumor
PHD	Prolil hidroxilase
PPARs	Receptores ativados por proliferadores de peroxissomo
PPAR $\gamma$	Receptor ativado por proliferadores de peroxissomo $\gamma$
PPRE	Elemento de resposta do proliferador de peroxissomo
RMN de $^1\text{H}$	Ressonância magnética nuclear de hidrogênio
RMN de $^{13}\text{C}$	Ressonância magnética nuclear de carbono
RXR	Receptor retinoide-X
TET	Translocação de dez-onze metilcitosina dioxigenase (em inglês: <i>ten-eleven translocation methylcytosine dioxygenase</i> )
TMZ	Temozolomida (em inglês: <i>temozolomide</i> )
TZD	2,4-tiazolidinediona (anel heterocíclico) (em inglês: <i>2,4-thiazolidinedione</i> )
TZDs	Tiazolidinedionas (derivados do anel da 2,4-tiazolidinediona) (em inglês: <i>thiazolidinediones</i> )

VEGF	Fator de crescimento do endotelial vascular
VEGFR	Receptor do fator de crescimento do endotelial vascular
$\alpha$ -KG	$\alpha$ -cetoglutarato

## SUMÁRIO

1. INTRODUÇÃO	17
2. OBJETIVOS	19
2.1. OBJETIVO GERAL	19
2.2. OBJETIVOS ESPECÍFICOS 1	19
2.3. OBJETIVOS ESPECÍFICOS 2	20
3. REVISÃO DA LITERATURA	21
3.1 GLIOMA	21
3.1.1 MUTAÇÃO IDH 1 / 2	23
3.1.2 CODELEÇÃO 1p/19q	24
3.1.3 G-CIMP	24
3.2 METILAÇÃO DO PROMOTOR DA MGMT	26
3.3 MECANISMOS DE AÇÃO DE FÁRMACOS ANTIGLIOBlastoma	27
3.4 POSSÍVEIS MECANISMOS DE AÇÃO ATITUMORAL DAS TZDs	30
3.5 TIAZOLIDINEDIONAS	34
3.5.1 SÍNTESE DAS TZDs	35
3.6 DERIVADOS DA TZD COM ATIVIDADE ANTIGLIOBlastoma	37
3.7 COMPOSTOS CONTENDO O HETEROCICLO TIAZOLIDINONA COM ATIVIDADE ANTIGLIOBlastoma	4- 38

4. RESULTADOS	39
4.1 ARTIGO	39
4.2 MANUSCRITO	62
5. CONCLUSÃO	82
6. REFERÊNCIAS BIBLIOGRÁFICAS	84
7. ANEXOS	90
7.1 ANEXO A - COMITÊ DE ÉTICA EM EXPERIMENTAÇÃO ANIMAL DO ARTIGO E DO MANUSCRITO (CEEA 9219)	90
7.2 ANEXO B - COMPROVANTE DE PUBLICAÇÃO NA REVISTA MEDICINAL CHEMISTRY	91
7.3 ANEXO C - COMPROVANTE DE SUBMISSÃO DO MANUSCRITO NA REVISTA ARCHIVES OF PHYSIOLOGY AND BIOCHEMISTRY	92

## **1. INTRODUÇÃO**

O glioma são tumores cerebrais primários (FERLAY, J. et al. 2010; OSTROM, Q.T. et al. 2014), representando 81% dos tumores malignos do cérebro (OSTROM, Q.T. et al. 2014). A classificação atualizada da Organização Mundial da Saúde (OMS) de 2016 recomenda o diagnóstico molecular dos gliomas de acordo com o status mutacional da enzima isocitrato desidrogenase (IDH).

O glioblastoma é o tipo de glioma mais comum (OSTROM, Q.T. et al., 2019) que apresenta uma sobrevida baixa, geralmente inferior a dois anos (STUPP, R. et al., 2005; CECCARELLI, M. et al. 2016). A resposta do glioblastoma à radioterapia e quimioterapia é limitada. Nesse contexto, o estudo realizado por STUPP, R. et al. 2005 demonstrou que pacientes tratados com radioterapia tiveram uma sobrevida de 12,1 meses, enquanto que pacientes tratados com radioterapia mais temozolamida (TMZ) tiveram uma sobrevida de 14,6 meses, ou seja, a utilização de TMZ aumentou a sobrevida em apenas dois meses e meio. Outros medicamentos, dentre eles alguns anticorpos monoclonais, foram testados com o intuito de estabelecer novos protocolos terapêuticos, entretanto nenhuma intervenção farmacológica demonstrou alterar o curso da doença (RHUN, E.L. et al. 2019). Essas informações evidenciam a necessidade de medicamentos mais eficazes para o tratamento do glioblastoma. Diversos estudos demonstram a atividade anticâncer de agonistas de receptores ativados por proliferadores de peroxissomo (PPARs) (WU, K. et al. 2016; PESTEREVA, E. et al. 2012; YOUSEFNIA, S. et al. 2018), uma vez que os agonistas de um dos subtipos de PPAR, o PPAR $\gamma$ , possuam papéis-chave na proliferação, metástase, angiogênese, apoptose e imunomodulação através da ativação de vias de sinalização em diferentes células cancerígenas, bem como em células-tronco cancerígenas (YOUSEFNIA, S. et al. 2018).

As TZDs são agonistas do PPAR $\gamma$  e vêm demonstrando ação antitumoral em diferentes linhagens celulares (YOUSEFNIA, S. et al. 2018). A pioglitazona e a rosiglitazona são exemplos de TZDs, a primeira é comercializada no Brasil como agente hipoglicêmico e a segunda teve seu registro cancelado devido a

efeitos adversos cardiovasculares, conforme informado pela Agencia Nacional de Vigilância Sanitária. Esses medicamentos, bem como vários derivados da TZD, foram testados em diferentes linhagens celulares, entre elas, linhagens de glioma (METWALLY, K. et al. 2017; RÊGO, M.J.B.M. et al. 2014). Nesse sentido, a pioglitazona já demonstrou efeito antiglioma em um modelo de xenoenxerto (GROMMES, C. et al. 2013), assim como em um estudo de fase II, no qual um novo regime foi moderadamente ativo e bem tolerado em pacientes com gliomas de alto grau (HAU, P. et al. 2007).

Em virtude da baixa sobrevida proporcionada pelo principal medicamento utilizado na terapia do glioblastoma, assim como pelas tentativas frustradas em estabelecer novos protocolos para esse tipo de tumor cerebral, observa-se a necessidade de estudos bioquímicos e químicos para a síntese e análise da atividade antiglioblastoma de novos compostos tendo como precursor o heterociclo TZD.

O Laboratório de Química Aplicada à Bioativos (LaQuiABio) vem estudando a síntese e a atividade antiglioma de compostos contendo o heterocíclico 4-tiazolidinona, um heterociclo análogo da TZD (SILVA, D.S. et al., 2016; SILVEIRA, E.F. et al. 2017). A diferença entre a TZD e a 4-tiazolidinona é que a primeira possui duas carbonilas, uma na posição 2 e a outra na posição 4 do anel, enquanto a segunda apresenta apenas uma carbonila na posição 4, mantendo o núcleo central das estruturas semelhantes. Tendo em vista os trabalhos da literatura bem como os resultados promissores obtidos até o momento pelo nosso grupo de pesquisa, nessa tese focamos no efeito antiglioma *in vitro* e *in vivo* de compostos derivados do heterociclo TZD.

## 2. OBJETIVOS

### 2.1. OBJETIVO GERAL

O presente estudo tem como objetivo a síntese, caracterização e avaliação do potencial antiglioblastoma *in vitro* e *in vivo* de derivados da 2,4-tiazolidinediona, com o intuito de desenvolver moléculas simples e que possam se tornar uma alternativa viável e com menores efeitos colaterais, quando comparadas com os fármacos já conhecidos e em testes para o tratamento do glioblastoma.

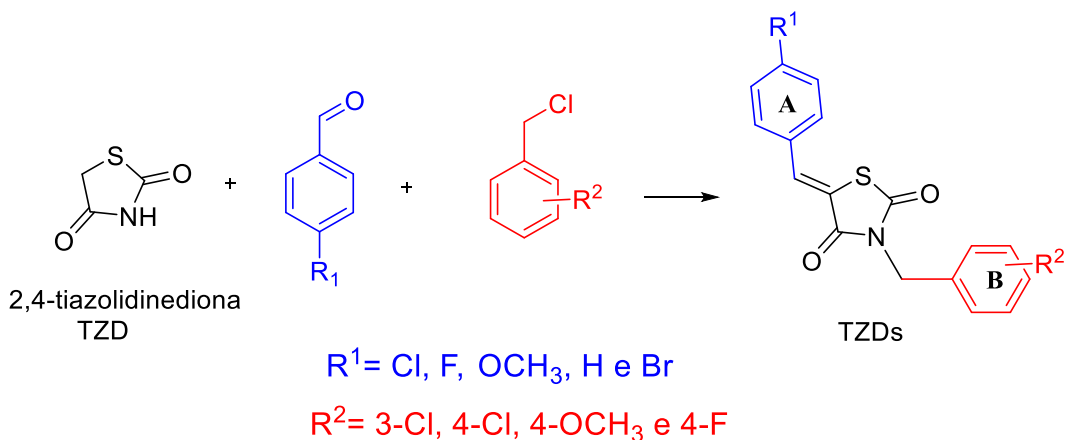
### 2.2. OBJETIVOS ESPECÍFICOS 1

Sintetizar uma série de 2,4-tiazolidinedionas funcionalizadas na posição 3 através da *N*-alquilação com cloretos de benzila substituídos e na posição 5 através da condensação aldólica (Knoevenagel) com benzaldeídos substituídos (Esquema 1).

Caracterizar as estruturas por CG-EM e RMN de  $^1\text{H}$  e  $^{13}\text{C}$ .

Avaliar, *in vitro*, a citotoxicidade dos derivados da 2,4-tiazolidinediona em linhagens celulares de glioblastoma de rato (C6) e de camundongo (GL261).

Avaliar, *in vitro*, a citotoxicidade dos derivados da 2,4-tiazolidinediona em cultura primária de astrócitos.



**Esquema 1.** Rota sintética para a obtenção das TZDs.

### **2.3. OBJETIVOS ESPECÍFICOS 2**

Avaliar a atividade antiglioma *in vivo* através da implantação de células de glioblastoma C6 em ratos Wistar e posterior tratamento com o(s) melhor(es) composto(s) do estudo *in vitro*.

Avaliação da função renal e hepática, bem como do perfil lipídico e conteúdo proteico no modelo pré-clínico de glioblastoma.

Avaliação comportamental no modelo pré-clínico de glioblastoma.

### **3. REVISÃO DA LITERATURA**

#### **3.1 GLIOMA**

Gliomas são tumores cerebrais primários que se acredita derivarem do tronco neuroglial ou células progenitoras (WELLER, M. et al. 2015). Os gliomas foram classificados de acordo com a Organização Mundial da Saúde de 2007, em uma escala ascendente de I a IV e nomeados de acordo com as células progenitoras (SAMUDRA, N. et al. 2019): (I) astrocitoma de células ciliadas; (II) astrocitoma difuso; (III) astrocitoma anaplásico, oligodendrogioma anaplásico e astrocitoma anaplásico; e (IV) glioblastoma (LIU, L. and LI, X. 2018).

A classificação atualizada da Organização Mundial da Saúde de 2016 recomenda o diagnóstico molecular do *status* mutacional da isocitrato desidrogenase (IDH). Os gliomas com IDH mutantes manifestam o fenótipo metilador da ilha de citosina-fosfato-guanina (CpG) (G-CIMP) (MALTA, T.M. et al., 2017). A classificação baseada na metilação do DNA, feita após uma grande análise genômica, refinou subgrupos anteriores de glioma com base na mutação da IDH e no status de codeleção 1p / 19q. Os subgrupos foram direcionados principalmente pelo status da mutação IDH 1 / 2 e classificados como: IDH-tipo selvagem e IDH-mutantes (CECCARELLI, M. et al. 2016) (Figura 1).

Os tumores IDH-tipo selvagem foram subdivididos nos tipos clássico, mesenquimal, LGm6-GBM e astrocitoma pilocítico. Os IDH-mutantes foram agrupados como codificadores e não codificadores de 1p / 19q e refinados em 2 subgrupos distintos, com base na extensão da metilação do DNA em G-CIMP baixo e G-CIMP alto, fornecendo um aprimoramento na classificação do glioma, independente do grau e da histologia (CECCARELLI, M. et al. 2016).

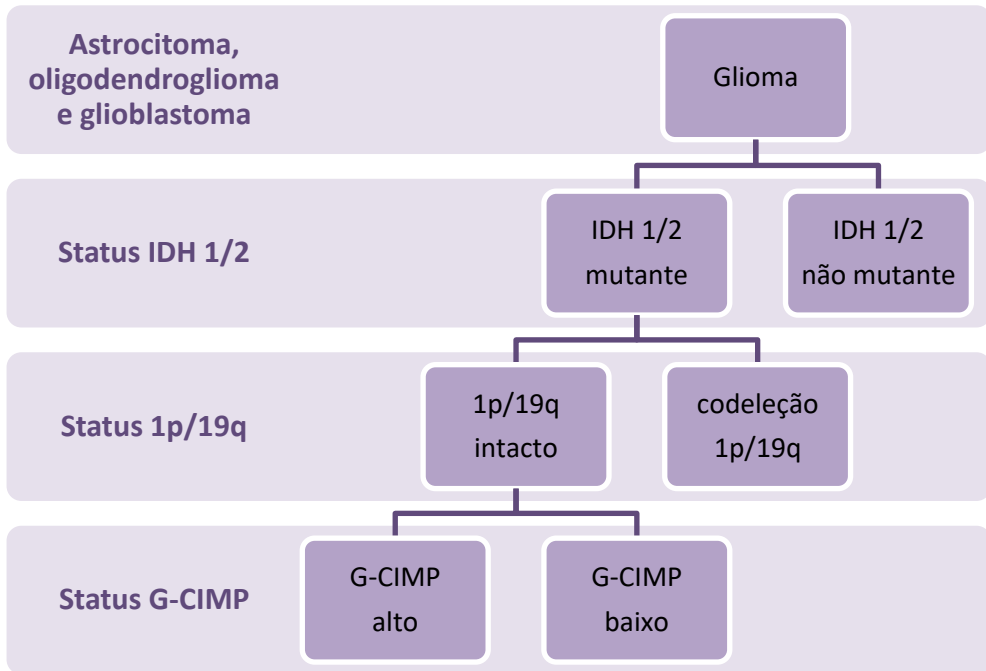


**Figura 1.** Critérios para classificação de gliomas (Adaptado de MALTA et al. 2017).

Mutação da enzima IDH, codeleção de 1p/19q, metilação do promotor da enzima O6-metilguanina-DNA metiltransferase (MGMT) e G-CIMP+ são biomarcadores prognósticos favoráveis independentes, ou seja, essas alterações são benéficas para os pacientes (MUR, P, 2015).

Cirurgia, radioterapia e quimioterapia com agentes alquilantes ainda são a base do tratamento, afetando enormemente a qualidade de vida dos pacientes. A cirurgia pode estar associada a déficits funcionais agudos, a radioterapia representa um grande risco de comprometimento neurocognitivo e a quimioterapia pode causar toxicidade hematológica e outras toxicidades (WELLER, M. et al. 2015).

Além do tratamento do próprio tumor, muitos pacientes requerem tratamento dos sintomas neurológicos associados, incluindo alterações cognitivas e comportamentais, fadiga e convulsões, os quais também afetam a qualidade de vida dos pacientes (SAMUDRA, N. et al 2019).

### 3.1.1 MUTAÇÃO IDH 1 / 2

A enzima IDH1 é responsável pela reação que transforma o isocitrato e o NADP+ em  $\alpha$ -cetoglutarato ( $\alpha$ -KG) e NADPH, essa reação ocorre no citosol da célula. Mutações nessa enzima levam a formação do ácido 2-hidroxipentérico (2-HG) a partir de  $\alpha$ -cetoglutarato ( $\alpha$ -KG) (Figura 3), reduzindo os níveis do  $\alpha$ -KG e aumentando os de 2-HG, resultando na inibição das enzimas de desmetilação de histona JHDM1, JMJD2 e 5 mC hidroxilase, que é da família das enzimas de translocação de dez-onze metilcitosina dioxigenase (TET). A inibição dessas enzimas causa hipermetilação de histonas. A enzima 5-metilpirimidina hidroxilase (5MPH) também é inibida, causando hipermetilação do DNA. Assim, a mutação da IDH pode afetar os padrões de metilação do DNA alterando a expressão de oncogenes, genes supressores de tumores ou outros componentes críticos e metabólicos da via (LIU, L. 2018) (Figura 2).

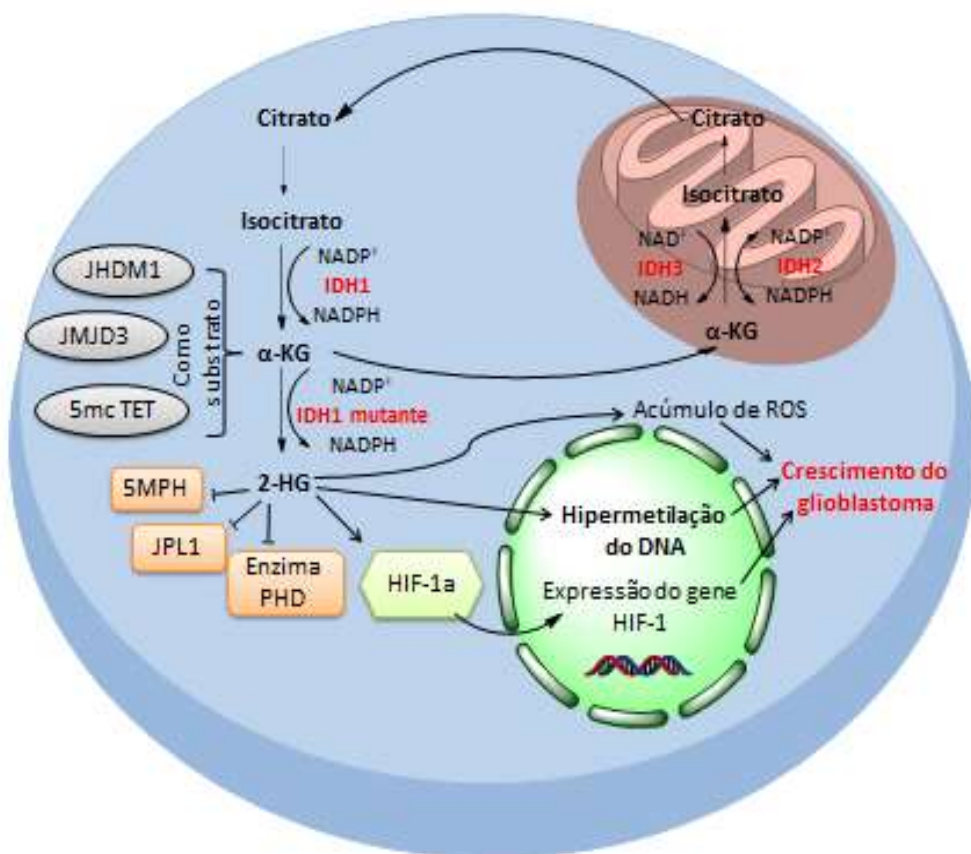


**Figura 2.** Mutação da IDH e sua relação com o ciclo do ácido tricarboxílico e vias que levam à tumorigênese após a mutação (Adaptado de LIU, L., 2018).

A figura 3 exemplifica uma das inibições enzimáticas citadas acima, o acúmulo de 2-HG inibe a enzima TET, desta forma não ocorre a desmetilação da 5-metilcitosina (5mC) e a 5-hidroximetilcitosina (5hmC) não é formada, ou seja, o DNA permanece metilado (Figura 3) (WU, H. 2011).

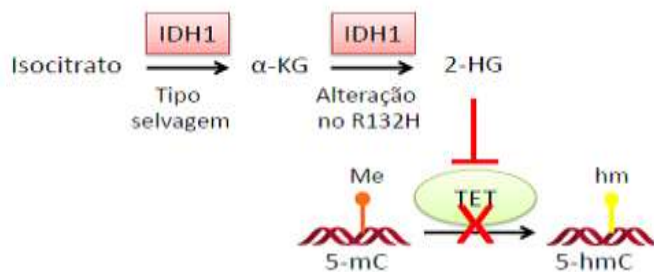


**Figura 3.** Inibição da enzima TET (Adaptado de WEISENBERGER, D.J. 2014).

O 2-HG também inibe a enzima prolil hidroxilase (PHD) a qual catalisa muitas reações, como o reparo do DNA alquilado, detecção de níveis de oxigênio e resposta a hipóxia (LIU, L. 2018). Os níveis aumentados de 2-HG também podem levar a ativação do fator induzível por hipóxia-1 (HIF-1), o qual está envolvido na regulação da expressão gênica no ambiente hipóxico, angiogênese, sobrevivência celular, metabolismo da glicose e transcrição de genes invasivos (ZHAO, S. et al. 2009). Além disso, as semelhanças estruturais entre 2-HG e glutamato indicam que o 2-HG pode ativar os receptores de glutamato nos neurônios, interferindo na homeostase intracelular do cálcio e na produção de espécies reativas de oxigênio (EROs) (LIU, L. 2018).

### 3.1.2 CODELEÇÃO 1p/19q

A codeleção 1p/19q provavelmente ocorre após uma translocação não equilibrada entre os braços dos cromossomos 1 e 19, levando a uma perda combinada de material genético (JENKINS, R.B. et al., 2006).

### 3.1.3 G-CIMP

O *status* de metilação do DNA resulta da ação das enzimas metilantes e/ou desmetilantes. A metilação do DNA é a transferência do grupo metil para a posição 5' do anel da citosina através da ação de uma enzima metilante,

levando a formação da 5mC (Figura 4), isso ocorre principalmente nos dinucleotídeos - CpG (GOLL, M.G. et al. 2005). Os CpGs dispersos por todo o genoma são geralmente metilados, a ilha de CpGs, localizada nas regiões promotoras, geralmente não é metilada (Figura 5). Em condições fisiológicas, a metilação da ilha de CpGs geralmente ocorre como um mecanismo de repressão genética em regiões específicas (DE CARVALHO, D.D. et al. 2010).

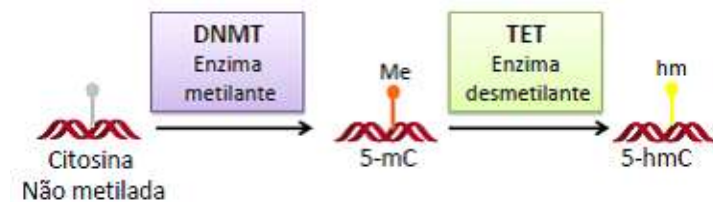


**Figura 4.** Metiltransferases de DNA (DNMTs) catalisando a transferência do grupo metil para a 5' citosina e desmetilação de 5mC pela enzima TET (Adaptado de WEISENBERGER, D.J. 2014).

No câncer, a metilação do DNA se torna aberrante e é caracterizada principalmente por hipermetilação em torno dos promotores dos genes e corpos gênicos e hipometilação entre elementos não promotores (Figura 5). A hipermetilação do promotor é um importante mecanismo de silenciamento epigenético dos genes supressores de tumores (MALTA, T.M. et al. 2017).

Com base na extensão da metilação global do DNA, descobriu-se dois subconjuntos de gliomas IDH-mutantes/G-CIMP+: um que apresenta baixo grau de metilação do DNA e pior resultado (G-CIMP-baixo); e outro que descreve alta metilação do DNA e melhores resultados (G-CIMP-alto) (Figura 1). Essa classificação reflete um refinamento do diagnóstico de tumores, integrando as características genotípicas e fenotípicas e estreitando os subgrupos definidos. Esse esquema pode ser útil para prever o resultado do paciente e tornar as estratégias terapêuticas mais eficazes e adaptadas a cada paciente (MALTA, T.M. et al., 2017).

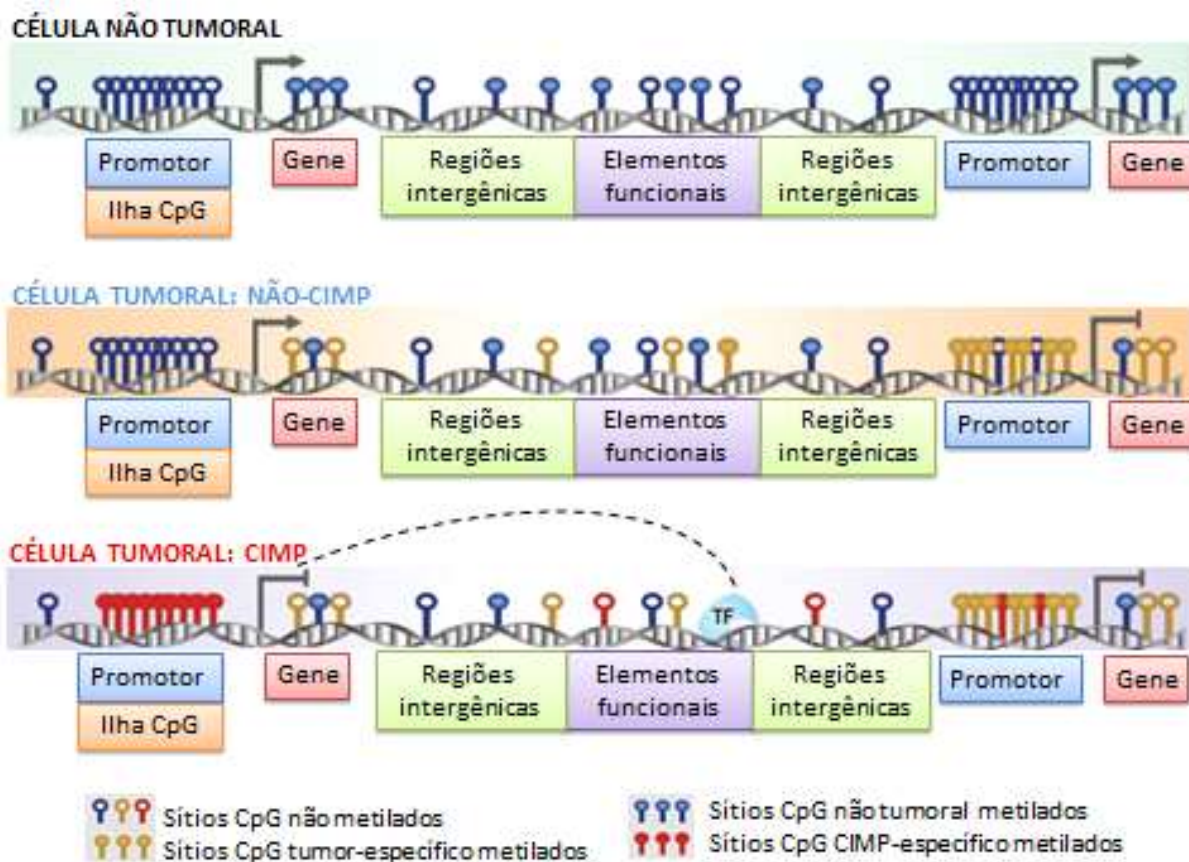


**Figura 5.** Alterações aberrantes da metilação do DNA em locais genômicos específicos em células tumorais (Adaptado de MALTA et al. 2017).

### 3.2 METILAÇÃO DO PROMOTOR DA O6-METILGUANINA-DNA METILTRANSFERASE (MGMT)

A MGMT é uma enzima de reparo de DNA que interfere na ação da TMZ. Essa enzima atua transferindo o grupo metil da posição O6 da guanina do DNA para a sua própria cisteína, o que repara os danos letais ao DNA induzido pela TMZ, permitindo que a célula tumoral sobreviva (Figura 6A) (JIAPAER et al. 2018).

Os níveis de expressão da MGMT correlacionam-se diretamente com o *status* da metilação da ilha CpG do promotor do gene da MGMT, ou seja, quando o promotor está metilado ocorre diminuição da expressão da MGMT e quando ele não está metilado a enzima é expressa normalmente.

Casos de glioblastoma com o promotor da MGMT metilado (Figura 6B) mostraram sobrevida prolongada em comparação a casos em que o promotor não estava metilado. Portanto, a enzima MGMT contribui para a resistência à TMZ (JIAPAER, S. et al. 2018)

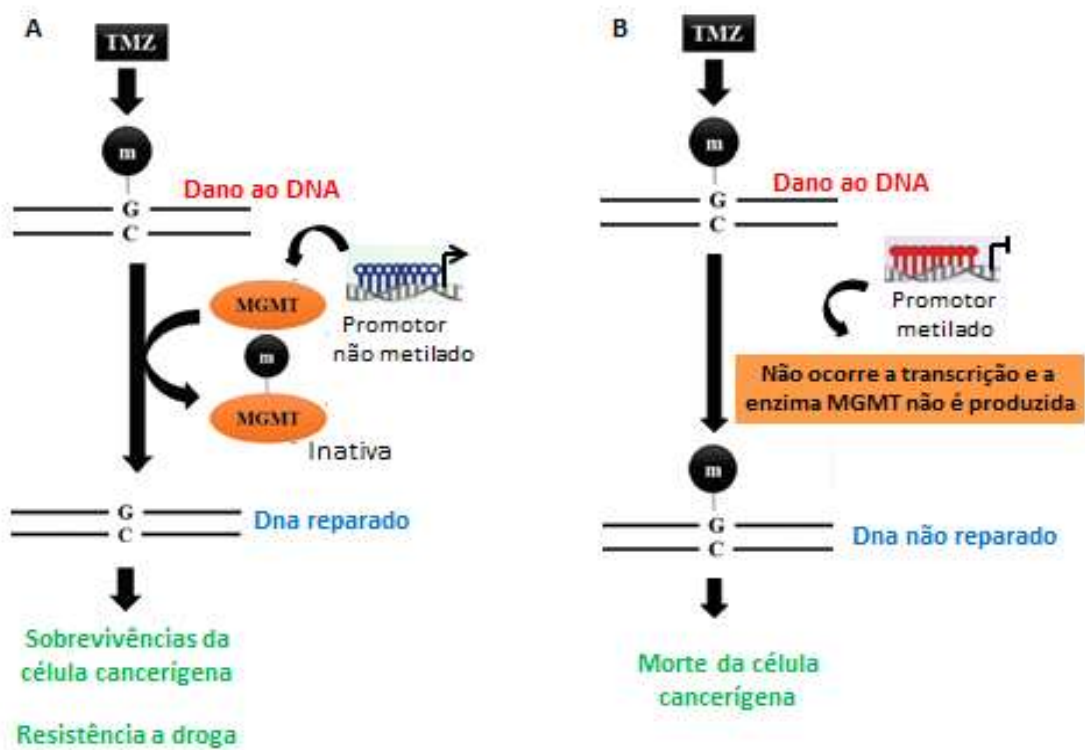


**Figura 6.** A) Desmetilação do DNA causada pela enzima MGMT e resistência à TMZ. B) Metilação do promotor do gene da enzima MGMT contribuindo para a ação da TMZ (Adaptado de JIAPAER et al. 2018).

### 3.3 MECANISMOS DE AÇÃO DE FÁRMACOS ANTIGLIOBLASTOMA

A maioria dos ensaios clínicos aborda a sinalização oncogênica via receptores de tirosina cinases, controle do ciclo celular e suscetibilidade à indução de apoptose. Na revisão publicada por RHUN et al. 2019, vários fármacos que foram testados em estudos de fase II e que atuam nas vias celulares frequentemente alteradas no glioblastoma, como a PI3K/AKT/mTOR, a proteína de tumor (p53) e a do receptor do fator de crescimento epidérmico (EGFR) falharam na melhora dos resultados terapêuticos (RHUN, E.L. et al. 2019).

Com exceção do fator de crescimento endotelial vascular (VEGF) - bevacizumabe, que prolongou a sobrevida sem progressão, mas não a sobrevida global, nenhuma intervenção farmacológica demonstrou alterar o curso da doença, e a quimioterapia com TMZ é ainda considerada o tratamento padrão de glioblastoma desde 2005 (RHUN et al. 2019).

O mecanismo de ação de fármacos que atuam no EGFR e no VEGF são ilustrados na figura 7. A ativação do EGFR leva a proliferação, invasão e resistência à indução de apoptose. O fármaco EGFR TKI inibe esse receptor, impedindo a ativação da proliferação (Figura 7A). O depatuxizumabe mafodotin, um anticorpo monoclonal associado a uma toxina, atua de outra forma, após a sua ligação ao EGFR, ocorre a internalização do anticorpo com posterior liberação da toxina, levando também a uma inibição da proliferação celular (Figura 7A) (BRENNAN, C.W. et al. 2013; FELSBERG, J. et al. 2017; RHUN et al. 2019).

A figura 7B ilustra o mecanismo de ação dos medicamentos bevacizumabe e cediranibe. O anticorpo monoclonal bevacizumabe se liga ao VEGF enquanto o fármaco cediranibe atua inibindo o receptor do VEGF (VEGFR), nos dois casos as vias intracelulares que levam a proliferação e angiogênese não são ativadas (PLATE, K.H. et al. 1994; SZABO, E. et al. 2016; RHUN et al. 2019).

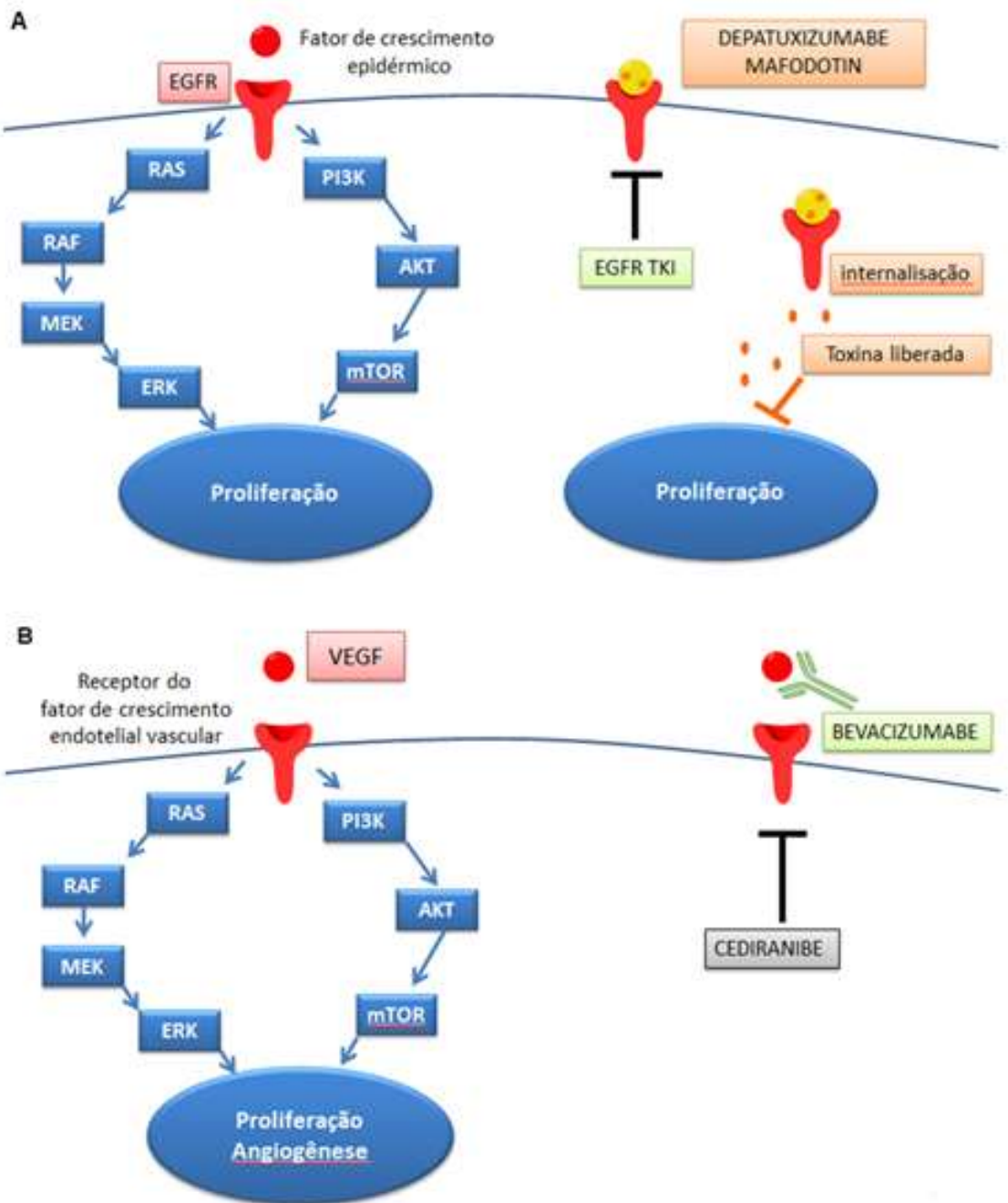


**Figura 7.** A) Mecanismo de ação dos fármacos EGFR TKI e depatuxizumabe mafodotin B) Mecanismo de ação dos fármacos bevacizumabe e cediranibe (Adaptado de RHUN et al. 2019).

### **3.4 POSSÍVEIS MECANISMOS DE AÇÃO ANTITUMORAL DAS TZDs**

Em virtude dos resultados clínicos não satisfatórios citados acima e da baixa sobrevida global proporcionada pelo principal medicamento antiglioblastoma - TMZ, estudos *in vitro* tem sido realizados com o intuito de analisar compostos mais eficazes e com diferentes mecanismos de ação, como, por exemplo, as TZDs. Esses compostos podem atuar de diferentes maneiras, como, por exemplo, através da ativação do receptor PPAR $\gamma$  (ZANDER, et al. 2002), aumento da expressão do transportador excitatório de aminoácidos 2 (EAAT2) (CHING, J. et al. 2015), inibição do receptor de IGF-1 (IGF -1R) (LIU, X. et al. 2010), entre outros (YOUSEFNIA, S. et al, 2018).

Os PPARs são receptores nucleares (FERRE, P. et. al. 2004), o subtipo PPAR $\gamma$  é expresso em vários tipos celulares neuronais, incluindo microglia, astrócitos, oligodendrócitos e neurônios (CHING, J. et al. 2015). Esse receptor é distribuído em uma variedade de células cancerígenas, dentre elas o glioblastoma (MOROSETTI, R. et al. 2004), possuindo agonistas naturais e sintéticos como por exemplo as TZDs, pioglitazona, rosiglitazona, troglitazona e ciglitazona (YOUSEFNIA, S. et al, 2018).

Após a ativação por ligantes, o PPAR $\gamma$  forma um heterodímero com o receptor retinoide-X (RXR), e esse complexo liga-se ao elemento de resposta do proliferador de peroxissoma (PPRE) dos genes alvo para induzir a transativação do sinal (Figura 8). Esse receptor regula o metabolismo da gordura, a homeostase energética, a proliferação e a inflamação (MOROSETTI, R. et. al. 2004).

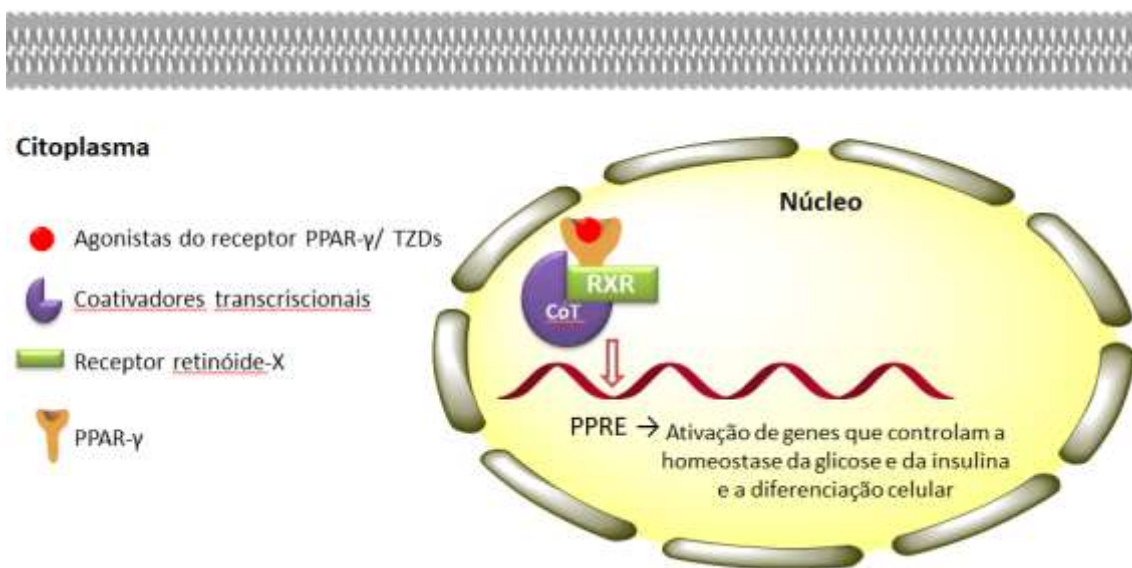


**Figura 8.** Ativação de genes via PPAR $\gamma$  (Adaptado de GROMMES, C. et al. 2004).

O estudo realizado por ZANDER, et al. 2002 demonstrou que células C6 de glioblastoma incubadas com 30  $\mu$ M de ciglitazona aumentam a expressão das proteínas pró-apoptóticas BAX e BAD, portanto um possível mecanismo de ação antiglioblastoma das glitazonas seria o aumento da expressão de proteínas pró-apoptóticas através da ativação do PPAR $\gamma$ . As proteínas BAX e BAD são expressas quando ocorre ativação dos seus respectivos genes. A indução da apoptose causada pelo PPAR $\gamma$  também pode ocorrer através da diminuição da atividade de p-p85, p-Akt, redução da expressão de Bcl2 ou supressão da via PI3K/Akt (YOUSEFNIA, S. et al. 2018).

Em geral, o envolvimento de ligantes do PPAR $\gamma$  na tumorigênese sugere que eles possuem potencial terapêutico isoladamente ou em combinação com outros medicamentos anticâncer (YOUSEFNIA, S. et al. 2018). Nesse contexto, GROMMES, C. et al. 2010 mostraram que pacientes diabéticos com glioblastoma que foram tratados com agonistas do PPAR $\gamma$  exibiram uma sobrevida média aumentada de 19 meses em comparação com pacientes que receberam o tratamento padrão para glioblastoma, para os quais a sobrevida mediana foi de 6 meses.

Outro mecanismo de ação antiglioblastoma estudado é o aumento da expressão do EAAT2 em células que possuem uma redução desse transportador, como nas células U87MG de glioblastoma (CHING et al. 2015). O EAAT2 é responsável por até 90% da captação extracelular de glutamato para o interior das células gliais. Após o glutamato ser transportado para o interior dessa célula esse é trocado, através do trocador Xc, por cisteína extracelular (YE, Z.C., 1999). A captação intracelular de cisteína via sistema Xc permite a sobrevivência das células do glioma através da formação da glutationa, a qual protege a célula contra as espécies reativas endógenas de oxigênio (CHUNG, W.J., 2005) (Figura 9)

As linhagens celulares de glioblastoma, assim como outras linhagens de glioma, expressam baixos níveis do EAAT2. O número reduzido desse transportador resulta em concentrações extracelulares anormalmente altas de glutamato, gerando excitotoxicidade, que causa necrose do parênquima adjacente e contribui para a proliferação (CHING, J. et al., 2015).

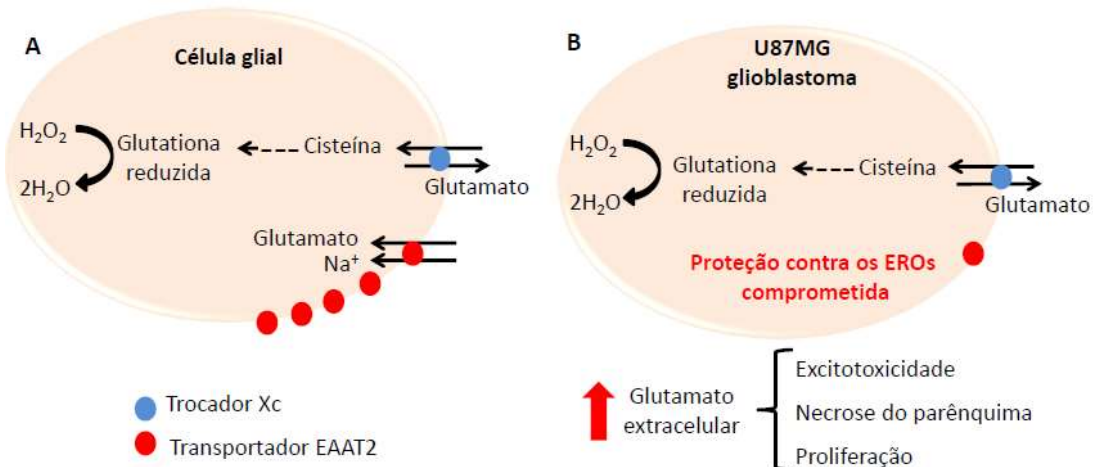


**Figura 9.** A) Trocador Xc e captação de glutamato extracelular através do EAAT2. B) Redução da expressão do EAAT2 e consequente aumento de glutamato extracelular e suas implicações (Adaptado de CHING et al. 2015).

O estudo realizado por CHING et al. 2015 verificou que a pioglitazona aumenta a expressão do EAAT2 em células U87 e reduz os níveis extracelulares de glutamato, possuindo, portanto, um efeito antiproliferativo. Além disso, o antagonista do PPARy GW9662 inibiu o efeito da pioglitazona

nos níveis extracelulares de glutamato, indicando dependência do receptor PPAR $\gamma$ . A pioglitazona também reduziu significativamente a viabilidade celular das células U87MG (30-100  $\mu$ M) e U251MG (100  $\mu$ M). O efeito na viabilidade foi parcialmente dependente da ativação do PPAR $\gamma$  nas células U87MG, mas não nas células U251MG (CHING, J. et al., 2015).

Além desse mecanismo de ação antiproliferativo, proposto para a pioglitazona, estudos demonstram que agonistas do PPAR $\gamma$  podem aumentar ou diminuir a proliferação de células cancerígenas de diferentes linhagens através da regulação da expressão de fatores proliferativos como: o fator nuclear Kappa  $\beta$ , a p38MAPK, a ciclina D, o receptor para produtos de glicação avançada e os inibidores das cinase dependente de ciclina ou cinase 4 dependente de ciclina (YOUSEFNIA, S. et al, 2018).

Derivados da TZD também demonstraram a capacidade de inibir os receptores do fator de crescimento tipo insulina (IGF-1R) (LIU, X. et al. 2010; MUGHAL, A. et al. 2015), os quais são importantes para a captação de glicose em astrócitos (FERNANDEZ, A.M. et al. 2017) e desempenham um papel central nas vias de sinalização que envolvem crescimento celular, proliferação e apoptose (LIU, X. et al. 2010). O IGF-1R possui uma forte atividade anti-apoptótica e a regulação negativa desse receptor leva à apoptose maciça de células cancerígenas (BASERGA, R. et al. 2003).

IGF-1R é altamente relacionado ao receptor de insulina (IR), uma vez que quando ocorre a ligação simultânea da insulina ao seu receptor e do fator de crescimento tipo insulina (IGF-1) ao seu receptor, há um aumento da captação de glicose em astrócitos (FERNANDEZ, A.M. et al. 2017). Nas células tumorais há uma alta expressão dos IGF-1R (LIU, X. et al. 2010), o que possibilita o aumento da captação de glicose e redução do dano oxidativo. As células tumorais captam mais glicose do que as células normais porque realizam mais a glicólise anaeróbica do que a aeróbica, isso ocorre para que haja uma redução dos níveis de espécies reativas produzidas durante a fosforilação oxidativa da glicólise aeróbica (LIU, X. et al. 2010; MOVAHEDA, Z.G. et al. 2019), logo, supõem-se que inibidores dos IGF-1R reduzam a

captação de glicose pela célula tumoral as deixando mais suscetíveis ao dano oxidativo.

### 3.5 TIAZOLIDINEDIONAS

A TZD é um anel heterocíclico de cinco membros com dois grupos carbonila nas posições dois e quatro (NAPOLEON, 2016). O anel pode ser funcionalizado nas posições cinco e três por meio de reações de condensação aldólica e reações de *N*-alquilação, respectivamente (Figura 10), permitindo o desenho e síntese de inúmeros derivados com potencial ação biológica (RADI, M. et al. 2010).

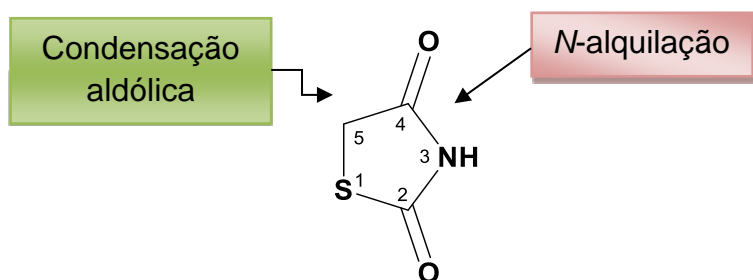


**Figura 10.** Estrutura da 2,4-tiazolidinediona e posições de funcionalização.

Em relação à atividade antitumoral, pesquisas sugerem que a ação das TZDs, também denominadas glitazonas, é altamente complexa, envolvendo uma variedade de efeitos genômicos e não genômicos, sendo que vários efeitos antitumorais ocorrem independentemente do PPAR $\gamma$  (FRÖHLICH, E. 2015). Por exemplo, a ciglitazona (Figura 11A) medeia a apoptose das células do glioma independentemente do PPAR $\gamma$  através da redução de Akt e indução da perda de potencial da membrana mitocondrial (LEE, M.W. et al., 2012) e a pioglitazona (Figura 11B) reduz a expressão da  $\beta$ -catenina independentemente do PPAR $\gamma$ . (WAN, Z. et al., 2011). Os efeitos são específicos para espécies e células e dependem da dose (FRÖHLICH, E. 2015).

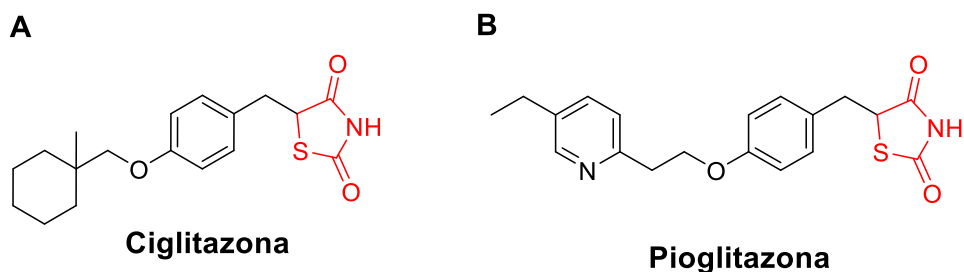
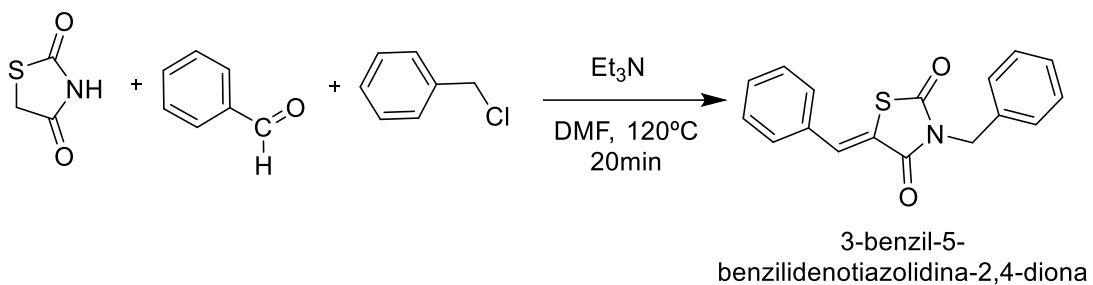


**Figura 11.** A) Estrutura química da ciglitazona. B) Estrutura química da pioglitazona.

### 3.5.1 SÍNTESE DAS TZDs

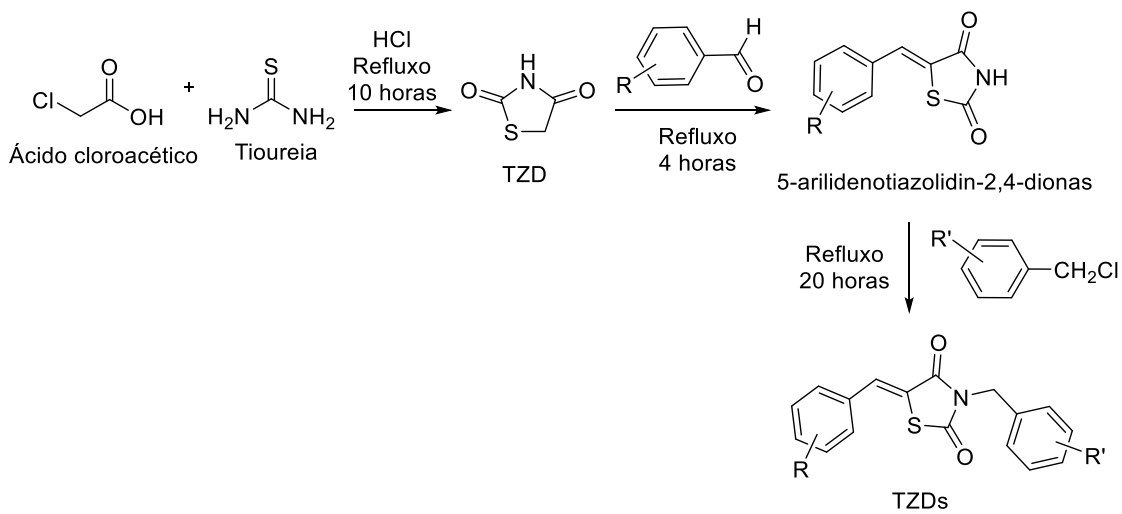
As reações de condensação aldólica e *N*-alquilação que levam a produção de derivados da TZD podem ser realizadas em apenas uma etapa (RADI, et al. 2010) ou em várias etapas (PUROHIT, S.S. et al. 2012) e através de diferentes metodologias (PRASHANTHA KUMAR, et al. 2006; PUROHIT, S.S. et al. 2012). A seguir serão descritas diferentes metodologias de síntese de TZDs.

Radi e colaboradores (RADI, et al. 2010) para sintetizar o composto 3-benzil-5-benzilidenotiazolidina-2,4-diona seguiram um protocolo já estabelecido por PRASHANTHA KUMAR, et al. 2006, no qual as TZDs são sintetizadas de maneira *one-pot* em micro-ondas (Esquema 2). Conforme o protocolo, para 0,171 mmol da tiazolidina-2,4-diona deve-se adicionar 0,5 mL de dimetilformamida (DMF), 0,342 mmol de trietilamina ( $\text{Et}_3\text{N}$ ), 0,205 mmol de cloreto de benzila e 0,342 mmol do benzaldeído, a mistura resultante é aquecida a 120°C em micro-ondas por 20 minutos (Esquema 2). Segundo os autores, o produto desejado foi obtido com rendimento de 70%. Esse procedimento obteve resultados comparáveis aos relatados por YANG, et al. 2003 em termos de rendimento e tempo reacional (20 minutos).



**Esquema 2.** Síntese de 3-benzil-5-benzilidenotiazolidina-2,4-diona de maneira *one-pot* em micro-ondas (RADIL, et al. 2010).

Outra metodologia que pode ser empregada é a metodologia por aquecimento térmico convencional. Os autores sintetizaram uma série de TZDs através de três etapas reacionais (Esquema 3) (PUROHIT, S.S. et al. 2012). Na primeira etapa foi sintetizada a TZD através da reação entre o ácido cloroacético, a tioureia e HCl em refluxo de água. Na segunda etapa foi sintetizado os intermediários 5-ariildenotiazolidin-2,4-dionas em uma reação de Knoevenagel de diferentes aldeídos e da TZD em refluxo de etanol. Por fim, na terceira etapa foram obtidas as TZDs pela *N*-alquilação dos intermediários com cloretos de benzila substituídos em refluxo de etanol. O rendimento obtido para os produtos finais foi em média de 70%.



**Esquema 3.** Síntese de uma série de TZDs realizada em três etapas pelo método de aquecimento térmico convencional (PUROHIT, S.S. et al. 2012).

De acordo com o descrito acima se constata que ambas as metodologias proporcionaram praticamente os mesmos rendimentos. Além disto, a metodologia *one-pot* em micro-ondas, realizada por RADI, et al. 2010, possibilita uma síntese mais rápida e com menos trabalho laboratorial, entretanto a purificação dos compostos utiliza hexano, o qual é tóxico para o organismo. Em contrapartida, a metodologia realizada por PUROHIT, S.S. et al. 2012 requer várias horas de trabalho e utiliza solventes tóxicos como o tolueno e o ácido clorídrico, o qual também é corrosivo, entretanto o processo de purificação é mais simples e rápido e utiliza o álcool etílico como solvente, que é menos tóxico que o hexano. Ambas as metodologias possuem vantagens e desvantagens sendo importantes bases para construção de protocolos mais rápidos, eficazes e menos tóxicos.

### 3.6 DERIVADOS DA TZD COM ATIVIDADE ANTIGLIOBlastoma

No estudo realizado por RÊGO et al., 2014, foi analisada a citotoxicidade de três derivados de TZD (Figura 12). A estrutura LPSF/SF-13 demonstrou ser seletivamente citotóxica contra a linhagem de glioblastoma NG97 ( $IC_{50} = 73,73 \mu M$  no ensaio do MTT) sem ser tóxica para as células mononucleares obtidas do sangue periférico de indivíduos saudáveis. A presença do grupo 3-Br pode ter contribuído para a citotoxicidade. Os autores relataram que a apoptose foi a principal processo de morte celular induzido por esse composto, embora também induzisse a necrose. Além disto, o estudo de modelagem molecular mostrou que o LPSF/SF-13 teve boa afinidade pelo PPAR $\gamma$  e que o substituinte 4-NO<sub>2</sub> é capaz de interagir com um hidrogênio do receptor PPAR $\gamma$ , o que pode estar relacionado a sua atividade antitumoral.

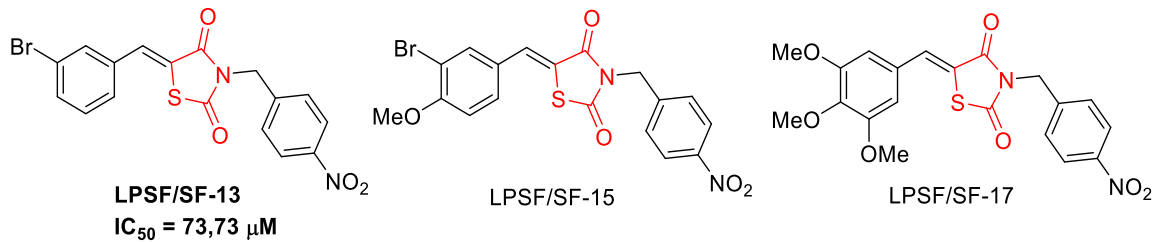


**Figura 12.** TZDs avaliadas no estudo de RÊGO et al. 2014.

### **3.7 COMPOSTOS CONTENDO O HETEROCICLO 4-TIAZOLIDINONA COM ATIVIDADE ANTIGLIOBLASTOMA**

Nosso grupo de pesquisa vem estudando compostos com atividade antiglioblastoma, especificamente estudos com compostos chamados 4-tiazolidinonas, os quais são análogos das TZDs.

O estudo realizado por SILVA et al., 2016 avaliou o potencial biológico de quatorze tiazolidin-4-onas. Neste trabalho seis compostos mostraram efeito significativo na redução da viabilidade celular em comparação com a droga padrão TMZ, na concentração de 100 µM em linhagem celular de ratos C6. Nenhum dos compostos mostrou toxicidade nas células primárias de astrócitos, demonstrando seletividade para as células tumorais.

SILVEIRA et al. 2017, também investigaram dezesseis estruturas sintéticas 2-aryl-3-((piperidin-1-il)etil)tiazolidin-4-onas. Treze dessas moléculas reduziram a viabilidade das células de glioma (C6) em 30-65% na concentração de 100 µM, no ensaio do MTT. Os quatro compostos mais promissores promoveram uma redução na viabilidade das células C6 superior a 50% e induziram a morte celular principalmente por mecanismos de necrose e apoptose tardios. Nenhum dos compostos foi citotóxico para os astrócitos, indicando seletividade para as células de glioma. Três desses foram testados *in vivo*, da seguinte forma: as células de glioma foram implantadas por injeção intracraniana em ratos Wistar adultos, os animais foram tratados com os compostos na dose de 5 mg/kg/dia por 15 dias e os tratamentos reduziram o volume tumoral em 45-73%, quando comparados ao controle. É importante ressaltar que os compostos não causaram mortalidade ou toxicidade nos animais.

## **4. RESULTADOS**

Em virtude dos achados de RÊGO et al., 2014 e dos trabalhos anteriores do nosso grupo de pesquisa (SILVA, D.S. et al., 2016 e SILVEIRA, E.F. et al. 2017) verificamos que o núcleo da 2,4-tiazolidinediona possui potencial para a ação antiglioblastoma. Sendo assim, uma série de derivados da TZD foi planejada, sintetizada, caracterizada e testada *in vitro* e *in vivo*.

Os resultados dessa Tese estão apresentados na forma de um artigo e um manuscrito científico: 1) O primeiro artigo (aceito para publicação) apresenta a síntese e a caracterização de 17 compostos, bem como os resultados do ensaio do MTT em células de glioblastoma de ratos, de camundongos e cultivo primário de astrócitos; 2) O segundo manuscrito (submetido) apresenta os testes *in vivo* de redução do volume tumoral do composto mais promissor em um modelo pré-clínico de glioblastoma em ratos Wistar, apresenta a toxicidade renal e hepática e a influência do composto na locomoção e memória dos ratos.

As seções materiais e métodos, resultados, discussão e referências encontram-se nos próprios artigos e representam a íntegra desse estudo.

O artigo e o manuscrito estão estruturados de acordo com as revistas às quais foram publicados ou submetidos.

### **4.1 ARTIGO**

#### **2,4-Thiazolidinedione as precursor to the synthesis of compounds with anti-glioma activities in C6 and GL261 cells**

Publicado no periódico Medicinal Chemistry

<https://doi.org/10.2174/1573406416666200403075826>

A aprovação junto ao comitê de ética em experimentação animal (CEEA) autorizando a realização da pesquisa desenvolvida neste manuscrito encontra-se em anexo a esta tese (**ANEXO A**). O comprovante de publicação na revista pode ser conferido no **ANEXO B**.

## **2,4-Thiazolidinedione as precursor to the synthesis of compounds with anti-glioma activities in C6 and GL261 cells**

Alana de Vasconcelos<sup>a</sup>; Ana Júlia Zulian Boeira<sup>a</sup>; Bruna Bento Drawanz<sup>a</sup>; Nathalia Stark Pedra<sup>b</sup>; Natália Pontes Bona<sup>b</sup>; Francieli Moro Stefanello<sup>b</sup>; Wilson Cunico<sup>a\*</sup>

<sup>a</sup> Laboratório de Química Aplicada à Bioativos (LaQuiABio), Centro de Ciências Químicas, Farmacêuticas e de Alimentos, Universidade Federal de Pelotas, Campus Universitário s/n, Capão do Leão, RS, Brazil, CEP: 96010-900.

<sup>b</sup> Laboratório de Neuroquímica, inflamação e Câncer (Neurocan) Centro de Ciências Químicas, Farmacêuticas e de Alimentos, Universidade Federal de Pelotas, Campus Universitário s/n, Capão do Leão, RS, Brazil, CEP: 96010-900.

**Background:** Thiazolidinediones (TZDs) represent an important class of heterocyclic compounds that have versatile biological activities, including anticancer activity. Glioma is one of the most common primary brain tumors and it is responsible for most of the deaths caused by primary brain tumors. In the present work, 2,4-thiazolidinediones were synthesized via a multi-component microwave *one-pot* procedure. The cytotoxicity of compounds was analyzed *in vitro* using rat (C6) and mouse (GL261) glioblastoma cell lines and primary cultures of astrocytes.

**Objective:** This study aims to synthesize and characterize 2,4-thiazolidinediones and evaluate their antitumor activity.

**Method:** TZDs were synthesized from three components: 2,4-thiazolidinedione, arene-aldehydes, and aryl chlorides. The reactions were carried out inside a microwave and monitored using thin-layer chromatography (TLC). Compounds were identified and characterized using gas chromatography coupled to mass spectrometry (GC-MS) and hydrogen (<sup>1</sup>H-NMR) and carbon nuclear magnetic resonance spectroscopy (<sup>13</sup>C-NMR). The antitumor activity was analyzed using the 3-(4,5-dimethyl)-2,5-diphenyltetrazolium bromide (MTT) reduction test, in which cell viability was verified in the primary cultures of astrocytes and in rat and mouse glioblastoma cells exposed to the synthesized compounds. The cytotoxicity of all derivatives was analyzed at the 100 µM concentration, both in astrocytes and in the mouse and rat glioblastoma cell lines. The compounds that showed the best results, **4CI** and **4DI**, were also tested at concentrations 25, 50, 100, 175, and 250 µM to obtain the IC<sub>50</sub>.

**Results:** Seventeen TZD derivatives were easily obtained through *one-pot* reactions in 40 minutes with yields ranging from 12% to 49%. All compounds were cytotoxic to both glioblastoma cell lines without being toxic to the astrocyte primary cell line at 100  $\mu\text{M}$ , thus demonstrating a selective activity. Compounds **4CI** and **4DI** showed the best results in the C6 cells: IC<sub>50</sub> of 28.51  $\mu\text{M}$  and 54.26  $\mu\text{M}$ , respectively.

**Conclusion:** The compounds were not cytotoxic in astrocyte culture, demonstrating selectivity for malignant cells. Changes in both rings are important for anti-glioma activity in the cell lines tested. The structure **4CI** had the best anti-glioma activity.

**Keywords:** Thiazolidinedione, anti-glioma, astrocyte, *one-pot* reaction, Knoevenagel, microwave synthesis.

## **1. INTRODUCTION**

Glioma is one of the most common primary brain tumors [1], originally derived from progenitor cells or neuroglial stem. It is responsible for most of the deaths caused by primary brain tumors and is characterized by high morbidity and mortality [2]. Less than 3% of patients with glioma survive more than 5 years after diagnosis [3].

Surgery, radiotherapy, and chemotherapy with the alkylating agent is still the bases of treatment, which profoundly affects patients' quality of life: surgery may be associated with acute functional deficits; radiotherapy represents a great risk of neurocognitive impairment, and chemotherapy may cause hematological toxicity and other acute toxicities [2].

2,4-Thiazolidinedione (TZD) is a five-membered heterocyclic ring with two carbonyl groups at two and four positions [4]. The ring can be functionalized at positions five and three through aldolic condensation and *N*-alkylation reactions, respectively, enabling the synthesis of various derivatives [5].

TZDs are synthetic high-affinity ligands for peroxisome proliferator-activated receptor (PPAR $\gamma$ ) and are studied for a wide variety of biological activities [6], including antitumor activity [7]. Some compounds of this pharmacological class, i.e., glitazones, are marketed in Brazil as hypoglycemic agents, such as pioglitazone, troglitazone, and rosiglitazone. The latter had its registration canceled due to liver toxicity. These drugs, as well as various TZD derivatives, have been tested in several types of cancers, such as

gliomas, using different cell lines. Some glitazones, such as pioglitazone, have been tested in humans [8].

Regarding antitumor activity, research suggests that the action of TZDs is highly complex, involving a variety of genomic and non-genomic effects, and several antitumor effects occur independently of PPAR $\gamma$ . The effects are cell, species, and compound-specific and dose-dependent [8a, 9].

The antitumoral activities of some substituted TZDs have been described in the literature. However, only a few studies analyze the relationship between the structure and anti-glioma activity of TZD derivatives. Tests with drugs bearing a TZD nucleus are more related to the study of the mechanism of action of these molecules. In a study by Wang *et al.* [10], rosiglitazone suppressed the growth of the human glioma cell lines U87 and U251, and it was verified that this specific glitazone induces interruption of the cell cycle and apoptosis and suppressed the expression of TGF- $\beta$  and its TGF-R2 receptor. The ability of TZDs to result in cell death via apoptosis is already well reported by other studies [11]. According to Grommes *et al.* [12], pioglitazone reduced viability, induced cell death of LN-229 *in vitro*, and reduced the tumor volume, invasion, and proliferation in the glioma xenograft model in mice. In addition, a clinical phase II study was conducted to evaluate the activity of pioglitazone and rofecoxib; these drugs were given in combination with low dose chemotherapy (capecitabine or temozolomide) in patients with high-grade glioma, where the stabilization of the disease was observed in 4 of the 14 patients (29%), for more than 3 months. Thus, the study demonstrated that this regimen is moderately active and well-tolerated in patients with high-grade glioma [9].

Thus, the synthesis of new compounds is necessary to identify the modifications resulting in more effective bioactive compounds and fewer adverse effects. The aim of this study is the synthesis, identification, and characterization of TZDs and the evaluation of their cytotoxic activities against rat (C6) and mouse (GL261) glioma cell lines and astrocyte cells.

## **2. MATERIAL AND METHODS**

### **2.1 Chemistry**

The synthesis of 2,4-thiazolidinedione derivatives was performed according to the procedure described by Radi *et al.* [5] with some modifications (Scheme 1). The procedure was performed in a microwave (Discover CEM 300 W) according to the *one-pot* protocol. 15 mL of dimethylformamide (DMF), 3 mmol of 2,4-thiazolidinedione (**1**), 4.2 mmol of substituted benzaldehyde (**2A-E**), 4.2 mmol of substituted benzyl chloride (**3F-I**), and 6 mmol of triethylamine were mixed at 120 °C for 40 minutes, washed with distilled water, and extracted with ethyl acetate. The organic phase was washed with saturated sodium chloride, dried with magnesium sulfate ( $\text{MgSO}_4$ ), and filtered. The solvent was removed using the rotary evaporator, and purification was done by recrystallization from ethyl alcohol.

### **2.2 Mass Spectrometer**

Gas chromatograph coupled to the mass spectrometer, model: QP2010 SE; automatic injector. Column: L.D. 0.25 nm; length 30 m, pressure 14 psi. Model: System AOC-20i. Brand name: Shimadzu®. Using as heating program: initial temperature = 50 °C, 2 min; injector temperature = 250 °C; final temperature = 250 °C, 10 min (16 °C/min); detector temperature = 270 °C.

### **2.3 Nuclear Magnetic Resonance Spectrometers**

$^1\text{H}$ - and  $^{13}\text{C}$ -NMR spectra were obtained by a Bruker Advance III 600 Spectrometer (600.13 MHz for  $^1\text{H}$  and 150.62 MHz for  $^{13}\text{C}$ ) and a Bruker Ascend 400 MHz (400 MHz for  $^1\text{H}$  and 100 MHz for  $^{13}\text{C}$ ) in DMSO-d<sub>6</sub> with TMS as the internal parameter.

### **2.4 Single-crystal X-ray diffraction (SC-XRD)**

Single crystal of the compound **4AH** was obtained by slow evaporation of ethanol at 25 °C. Diffraction measurement was performed using a Bruker D8 VENTURE diffractometer using Mo K $\alpha$  radiation ( $\lambda = 0.71073\text{\AA}$ ) with a KAPPA four-circle goniometer equipped with a PHOTON II CPAD area detector. Anisotropic displacement parameters for non-hydrogen atoms were applied. The structure was solved by SHELXL program and refined based on the full-matrix least-squares method

using the SHELXL program [13]. The ORTEP projection of the molecular structure was generated using the ORTEP-3 program [14]. Crystallographic information file (CIF) is deposited at the Cambridge Crystallographic Data Centre (CCDC) under identification number 1877438.

## 2.5 Melting points

The melting points were determined on a Fisatom model 430, 230 V, 60 Hz, 50 W apparatus using a thermometer with a capacity of up to 360 °C.

## 2.6 General cell culture procedures

### 2.6.1 Glioma cultures

Rat C6 and mouse GL261 glioblastoma cell lines were obtained from American Type Cell Collection (Rockville, Maryland, USA). Cells were grown in culture flasks and maintained in Dulbecco's Modified Eagle's Medium (DMEM) (pH 7.4) containing 1% DMEM (Gibco BRL), 8.4 mM HEPES, 23.8 mM NaHCO<sub>3</sub>, 0.1% fungizone, 0.5 U/mL penicillin/streptomycin and supplemented with 10% FBS.

### 2.6.2 Primary astrocyte cultures

Astrocyte cultures were prepared as previously described by [15]. Briefly, the cortex of newborn Wistar rats (1–3 days old) was removed and dissociated mechanically in Ca<sup>+2</sup> and Mg<sup>+2</sup>-free balanced salt solution (CMF) (pH 7.4) containing 137 mM NaCl, 5.36 mM KCl, 0.27 mM Na<sub>2</sub>HPO<sub>4</sub>, 1.1 mM KH<sub>2</sub>PO<sub>4</sub>, and 6.1 mM glucose. Dissociated tissue was subjected to centrifugation at 1,000 g for 5 min. Thereafter, the pellet was suspended in DMEM (pH 7.6) supplemented with 10% FBS. Then, cells ( $5 \times 10^4$ ) were seeded in poly-L-lysine-coated 96-well plates. Cultures could grow to confluence by 15–20 days and the medium was replaced every 5 days. All procedures used in the present study followed the “Principles of Laboratory Animal Care” of the National Institutes of Health (NIH) and were approved by the Ethical Committee of UFPel (CEEA 9219).

## **2.7 In vitro cell culture treatment**

Seventeen 2,4-thiazolidinedione derivatives (**4AF-4AI – 4DF-4DI** and **4EH**) were first dissolved in 10 mM stock DMSO (stock solution) and then diluted in DMEM with 10% FBS to obtain 100 µM in the wells. For the calculation of IC<sub>50</sub>, the final concentration in the wells of compounds **CI** and **DI** was 25, 50, 100, 175 and 250 µM. Glioblastoma cell lines C6 and GL261 were seeded at 5 x 10<sup>3</sup> cells (96-well plates) for cytotoxicity experiments and allowed to grow for 24 h. Astrocyte cultures were prepared as described above. Cell cultures were treated with 2,4-thiazolidinedione derivatives **4AF-4AI – 4DF-4DI** and **4EH** (100 µM) for 72 h and compounds **4CI** and **4DI**, at concentrations of 25, 50, 100, 175 and 250 µM. Cells exposed to DMSO (final concentration of 0.05%) were considered control.

## **2.8 Cell viability assay**

Dehydrogenases-dependent 3-(4,5-dimethyl)-2,5-diphenyltetrazolium bromide (MTT) reduction was used to estimate the viability of glioma and astrocyte cell cultures as described by Mosmman [16]. This method is based on the ability of viable cells to reduce MTT to form a blue formazan product. MTT solution was added to the incubation medium in the wells at a final concentration of 0.5 mg/mL. The cells were left for 90 min at 37°C in a humidified 5% CO<sub>2</sub> atmosphere. The medium was then removed and the precipitate was eluted with DMSO. The optical density of each well was measured at 492 nm in a microplate reader (SpectraMAX 190). Results were expressed as a percentage of control.

## **2.9 Statistical analysis**

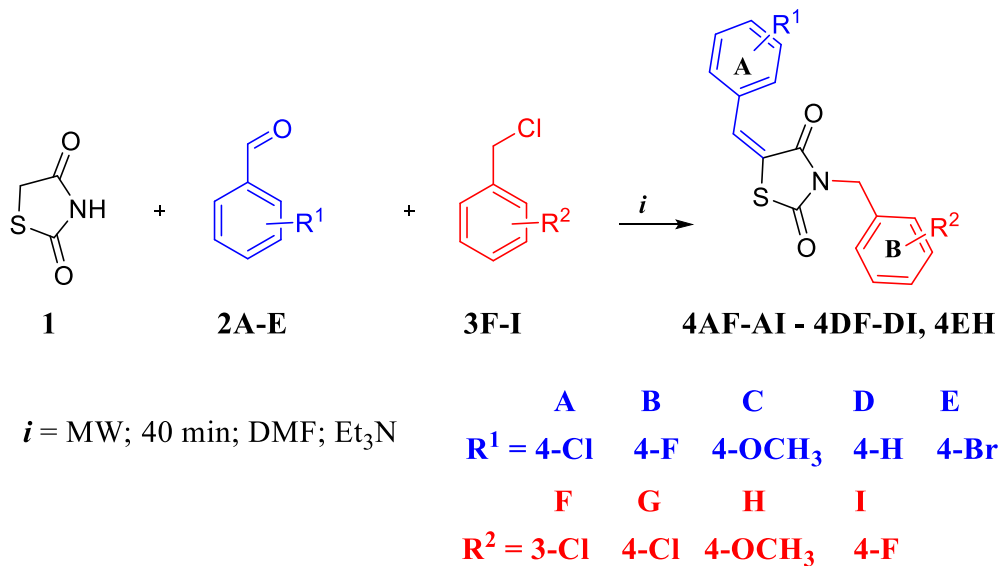
Results are expressed as means ± standard errors of the means. Statistical analyses were performed using one-way analysis of variance (ANOVA) followed by the Tukey *post-hoc* test. Differences were considered significant when associated with *P* values <0.05.

## **3. RESULTS AND DISCUSSION:**

### **3.1. Chemistry**

Recently, we reported the synthesis of 5-arylidene-2,4-thiazolidinediones via Knoevenagel reaction in a non-conventional sonochemistry method and obtained yields of 25–81% in 10–30 min reaction time [17]. Here, we employed the microwave method

to the multicomponent synthesis in a one-step procedure by two reactions: Knoevenagel and *N*-alkylation (**Scheme 1**).

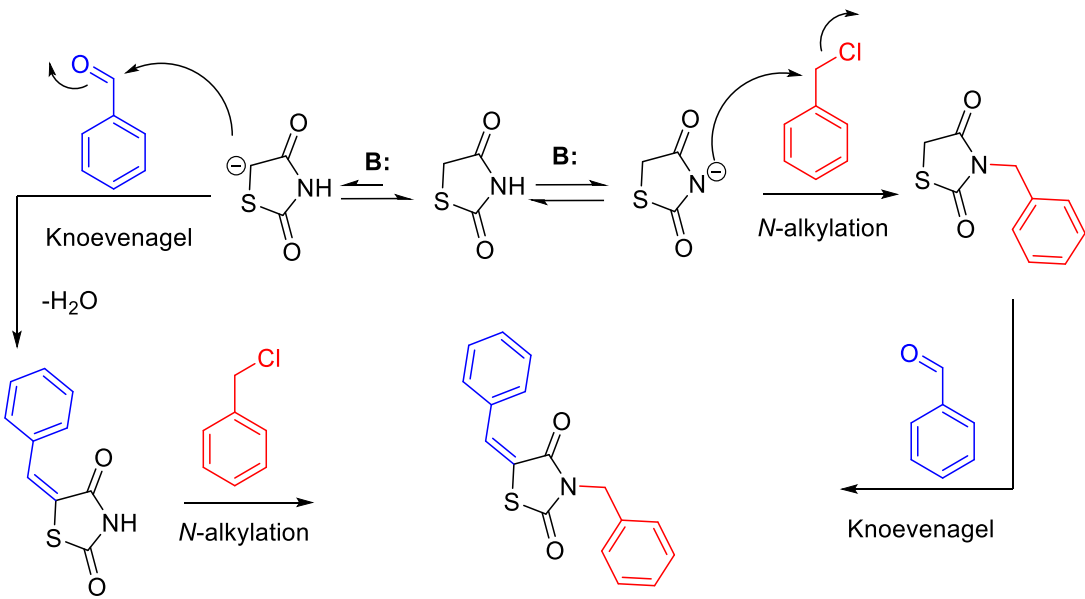


**Scheme 1.** *One-pot* synthesis of the desired 2,4-thiazolidinediones **4**.

The progress of the reactions was monitored by thin-layer chromatography (TLC) and higher reaction time was necessary to complete consumption of TZD (40 min.) than reported by Radi *et. al.* [5]. Although it was necessary to double the time, the use of the microwave and the *one-pot* methodology makes the procedure much faster as the conventional methods require (up to 72 hours) [18].

The purification process was also modified: Radi *et. al.* [5] performed by column, whereas, we employed recrystallization in ethanol. However, our yields ranged from 12–49%, which are less than that of Radi *et. al.* The change in the purification method used and the structural differences of the synthesized molecules may account for the lower yields.

In aldolic condensation, methylene at position five of the TZD ring reacts with the carbonyl of the substituted benzaldehydes (**2A-E**). In the *N*-alkylation reaction, the electron pairs of nitrogen attack the partially positive carbon of the substituted benzyl chloride (**3F-I**) in a classic SN<sub>2</sub> reaction. These reactions occur simultaneously in a multi-component microwave *one-pot* procedure (MO), as shown in **Scheme 2**.



**Scheme 2.** Pathway to the synthesis of TZDs.

The synthesized compounds were identified using gas chromatography (GC-MS),  $^1\text{H}$ -NMR, and  $^{13}\text{C}$ -NMR. The molecular structure for compound **4AH** was obtained by Single Crystal X-Ray Diffraction (SC-XRD) as it presents a monoclinic system and  $P2_1/c$  space group. The Ortep diagram for this structure is shown in **Figure 1**.

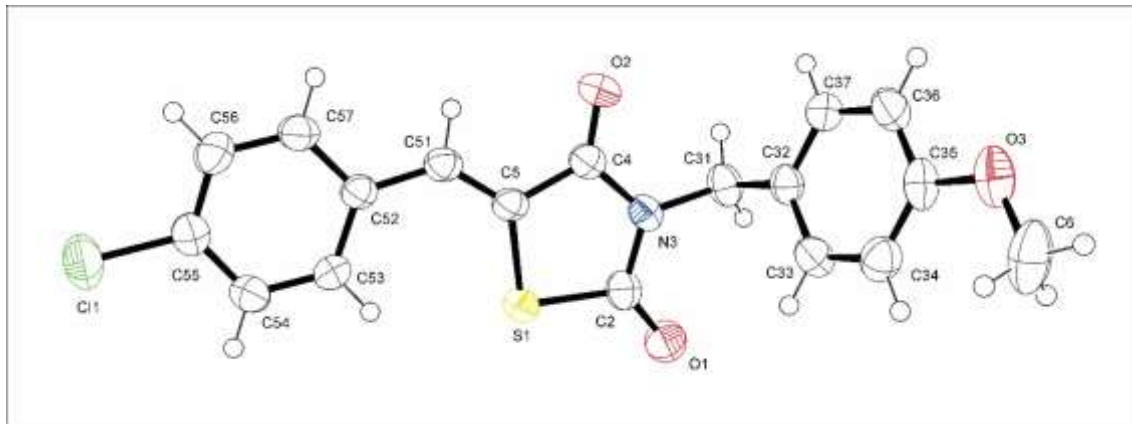


**Figure 1.** ORTEP diagram of **4AH**. Displacement ellipsoids are drawn at 50% probability level (green: chlorine; yellow: sulfur; red: oxygen; blue: nitrogen).

Two cleavage patterns, i.e., splitting of the nitrogen atom, were observed: from the benzyl group (**Figure 2a**, pattern 1) and from the fragment of the TZD ring (**Figure 2b**, pattern 2). The first pattern occurs due to the methoxy and fluoro substituents in the *para* position that stabilizes the benzylic carbocation B by resonance. The chlorine atom at this position also provides this stabilization in all structures except for **4DG**. The

chlorine substituent at the *meta* position on ring B does not stabilize the benzyl carbocation, and thus, another pattern cleavage was observed.

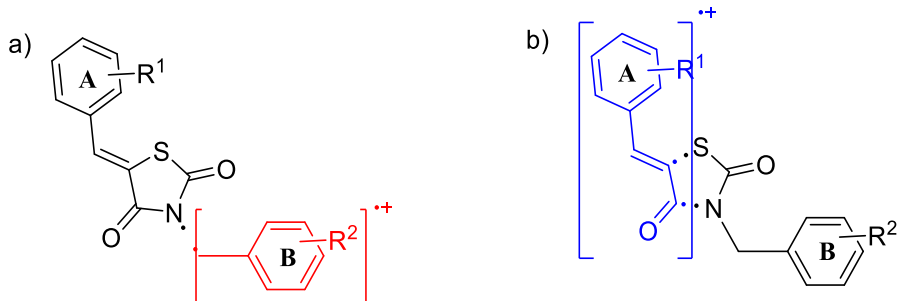


**Figure 2.** Structure fragmentation: (a) nitrogen of the TZD and methylene (pattern 1: AG, AH, AI, BG, BH, BI, CH, DH, DI, and EH), and (b) TZD ring fragmentation (pattern 2: AF, BF, CF, CG, CI, DF, and DG).

In the <sup>13</sup>C-NMR spectra, the carbonyl signals appear in the range of 164.9–167.5 ppm, the vinylic carbons between 131.9 and 133.5 ppm, and the methylenic carbons in the range of 43.8–44.8 ppm. In the <sup>1</sup>H-NMR spectra, the vinyl hydrogen appears as a singlet in the range of 7.91–7.97 ppm, and the methylenic hydrogens (CH<sub>2</sub>) also appear as a singlet in the range of 4.75–4.86 ppm. Additionally, the signals for aromatic carbons and hydrogen appeared in their characteristic regions in both NMR spectra, confirming the formation of desired compounds.

Eight of the 17 compounds synthesized are unpublished, namely, **4AF**, **4AH**, **4BF**, **4BH**, **4CH**, **4DF**, **4DH** and **4EH**; whereas, others are published, such as **4AG**, **4BG**, and **4DG** [19]; **4AI** and **4BI** [20]; **4CF** [21]; **4CG** [22]; **4CI** [23]; and **4DI** [24]. However, no anti-glioma studies were performed for the published compounds.

### 3-(3-chlorobenzyl)-5-(4-chlorobenzylidene)thiazolidine-2,4-dione; **4AF**

C<sub>17</sub>H<sub>11</sub>Cl<sub>2</sub>NO<sub>2</sub>S. Yield: 38%. Mp: 164–166 °C.

MS (70 eV): m/z (%): 363,05 (M<sup>+</sup>, 18), 168 (100), 89 (46), 125 (44).

<sup>1</sup>H-NMR (600 MHz, DMSO-d<sub>6</sub>) δ 4.85 (s, 2H, H11), 7.27 (d, J = 6.9 Hz, 1H, aryl B), 7.37–7.39 (m, 3H, aryl B), 7.61 (d, J = 8.6 Hz, 2H, aryl A), 7.65 (d, J = 8.6 Hz, 2H aryl A), 7.96 (s, 1H, H7).

<sup>13</sup>C-NMR (150 MHz, DMSO-d<sub>6</sub>) δ 44.0 (CH<sub>2</sub>, C11), 121.9 (C), 126.2 (CH, aryl B), 127.5 (CH, aryl B), 127.7 (CH, aryl B), 129.3 (2 CH, aryl A), 130.4 (CH, aryl B), 131.6 (2 CH, aryl A), 131.7 (C), 132.1 (CH, C7), 133.1 (C), 135.2 (C), 137.6 (C), 165.2 (C=O), 167.0 (C=O).

**3-(4-chlorobenzyl)-5-(4-chlorobenzylidene)thiazolidine-2,4-dione; 4AG [19]**

C<sub>17</sub>H<sub>11</sub>Cl<sub>2</sub>NO<sub>2</sub>S. Yield: 38%. Mp: 183–186°C.

MS (70 eV): m/z (%): 363 (M<sup>+</sup>, 20), 125 (100), 168 (65), 89 (30).

**5-(4-chlorobenzylidene)-3-(4-methoxybenzyl)thiazolidine-2,4-dione; 4AH**

C<sub>18</sub>H<sub>14</sub>ClNO<sub>3</sub>S. Yield: 26%. Mp: 154–156 °C.

MS (70 eV): m/z (%): 359 (M<sup>+</sup>, 6), 121 (100), 77 (5), 168 (5).

<sup>1</sup>H-NMR (600 MHz, DMSO-d<sub>6</sub>) δ 3.73 (s, 3H, OCH<sub>3</sub>), 4.77 (s, 2H, H11), 6.90 (d, J = 8.7 Hz, 2H, aryl B), 7.26 (d, J = 8.6 Hz, 2H, aryl B), 7.60 (d, J = 8.6 Hz, 2H, aryl A), 7.64 (d, J = 8.6 Hz, 2H, aryl A), 7.94 (s, 1H, H7).

<sup>13</sup>C-NMR (150 MHz, DMSO-d<sub>6</sub>) δ 44.2 (CH<sub>2</sub>, C11), 55.0 (OCH<sub>3</sub>, C18), 113.9 (2 CH), 121.9 (C), 127.3 (C), 129.2 (2 CH), 129.3 (2 CH), 131.6 (2 CH), 131.7 (C), 131.9 (CH, C7), 135.2 (C), 158.9 (C), 165.2 (C=O), 166.8 (C=O).

**5-(4-chlorobenzylidene)-3-(4-fluorobenzyl)thiazolidine-2,4-dione; 4AI [20]**

C<sub>17</sub>H<sub>11</sub>ClFNO<sub>2</sub>S. Yield: 31%. Mp: 176–178 °C.

MS (70 eV): m/z (%): 347 (M<sup>+</sup>, 20), 109 (100), 168 (35), 89 (10).

**3-(3-chlorobenzyl)-5-(4-fluorobenzylidene)thiazolidine-2,4-dione; 4BF**

C<sub>17</sub>H<sub>11</sub>ClFNO<sub>2</sub>S. Yield: 12%. Mp: 137–140 °C.

MS (70 eV): m/z (%): 347 (M<sup>+</sup>, 25), 152 (100), 125 (25), 89 (10).

<sup>1</sup>H-NMR (600 MHz, DMSO-d<sub>6</sub>) δ 4.86 (s, 2H, H11), 7.28 (d, J = 7.0 Hz, 1H, aryl B), 7.37–7.40 (m, 5H, aryl A and aryl B), 7.70 (dd, J = 8.7, 5.4 Hz, 2H, aryl A), 7.97 (s, 1H, H7).

<sup>13</sup>C-NMR (150 MHz, DMSO-d<sub>6</sub>) δ (ppm, J<sub>C-F</sub>= Hz) 44.0 (CH<sub>2</sub>, C11), 116.4 (d, <sup>2</sup>J = 22.1, 2CH, C2 e C6), 120.8 (d, J = 2.2, C, C8), 126.2 (CH, aryl B), 127.5 (CH, aryl B), 127.7 (CH do aryl B), 129.5 (d, <sup>4</sup>J = 3.1, C, C4), 130.4 (CH, aryl B), 132.3 (CH, C7), 132.5 (d, <sup>3</sup>J = 8.9, 2CH, C3 e C5), 133.1 (C), 137.6 (C), 162.9 (d, <sup>1</sup>J = 251.1, C, C1), 165.3 (C=O), 167.1 (C=O).

### **3-(4-chlorobenzyl)-5-(4-fluorobenzylidene)thiazolidine-2,4-dione; 4BG [19]**

C<sub>17</sub>H<sub>11</sub>ClFNO<sub>2</sub>S. Yield: 20%. Mp: 159–162 °C.

MS (70 eV): m/z (%): 347 (M<sup>+</sup>, 34), 125 (100), 152 (90), 89 (15).

### **5-(4-fluorobenzylidene)-3-(4-methoxybenzyl)thiazolidine-2,4-dione; 4BH**

C<sub>18</sub>H<sub>14</sub>FNO<sub>3</sub>S. Yield: 16%. Mp: 128–132 °C.

MS (70 eV): m/z (%): 343 (M<sup>+</sup>, 7), 121 (100), 152 (10), 77 (6).

<sup>1</sup>H-NMR (600 MHz, DMSO-d<sub>6</sub>) δ 3.72 (s, 3H, OCH<sub>3</sub>), 4.75 (s, 2H, H11), 6.90 (d, J = 8.7 Hz, 2H, aryl B), 7.25 (d, J = 8.6 Hz, 2H, aryl B), 7.37 (d, J = 8.8 Hz, 1H aryl A), 7.39 (d, J = 8.8 Hz, 1H, aryl A), 7.69 (dd, J = 8.6, 5.5 Hz, 2H, aryl A), 7.95 (s, 1H, H7).

<sup>13</sup>C-NMR (150 MHz, DMSO-d<sub>6</sub>) δ (ppm, J<sub>C-F</sub>= Hz) 44.3 (CH<sub>2</sub>, C11), 55.2 (OCH<sub>3</sub>, C18), 114.1 (2CH, aryl B), 116.6 (d, <sup>2</sup>J = 22.0 , 2 CH, C2 e C6 ), 120.9 (d, J = 2.2, C, C8), 127.5 (C), 129.5 (2CH, aryl B), 129.6 (d, <sup>4</sup>J = 3.1, C, C4), 132.4 (CH, C7), 132.73 (d, <sup>3</sup>J = 8.9, 2CH, C3 e C5), 159.0 (C), 163.1 (d, <sup>1</sup>J = 251.0, C1), 165.5 (C=O), 167.2 (C=O).

### **3-(4-fluorobenzyl)-5-(4-fluorobenzylidene)thiazolidine-2,4-dione; 4BI [20]**

C<sub>17</sub>H<sub>11</sub>F<sub>2</sub>NO<sub>2</sub>S. Yield: 38%. Mp: 152–154 °C.

MS (70 eV): m/z (%): 331 (M<sup>+</sup>, 27), 109 (100), 152 (50), 83 (10).

### **3-(3-chlorobenzyl)-5-(4-methoxybenzylidene)thiazolidine-2,4-dione; 4CF [21]**

C<sub>18</sub>H<sub>14</sub>ClNO<sub>3</sub>S. Yield: 42%. Mp: 147–150 °C.

MS (70 eV): m/z (%): 359 (M<sup>+</sup>, 28), 164 (100), 149 (30), 121 (10).

<sup>13</sup>C-NMR (150 MHz, DMSO-d<sub>6</sub>) δ 43.9 (CH<sub>2</sub>, C11), 55.4 (OCH<sub>3</sub>, C19), 114.9 (2 CH, aryl A), 117.7 (C), 125.3 (C, C4), 126.1 (CH, aryl B), 127.4 (CH, aryl B), 127.6 (CH,

aryl B), 130.4 (CH, aryl B), 132.1 (2 CH, aryl A), 133.1 (C, C12), 133.5 (CH, C7), 137.8 (C, C14), 161.2 (C, C1), 165.4 (C=O), 167.2 (C=O).

**3-(4-chlorobenzyl)-5-(4-methoxybenzylidene)thiazolidine-2,4-dione; 4CG [22]**

$C_{18}H_{14}ClNO_3S$ . Yield: 24%. Mp: 159–161 °C.

MS (70 eV): m/z (%): 359 ( $M^+$ , 34), 164 (100), 125 (40), 149 (35).

**3-(4-methoxybenzyl)-5-(4-methoxybenzylidene) thiazolidine- 2,4-dione; 4CH**

$C_{19}H_{17}NO_4S$ . Yield: 12%. Mp: 142–145 °C.

MS (70 eV): m/z (%): 355 ( $M^+$ , 13), 121 (100), 149 (7), 77 (7).

$^1H$ -NMR (400 MHz, DMSO-d<sub>6</sub>) δ 3.72 (s, 3H, OCH<sub>3</sub>), 3.83 (s, 3H, OCH<sub>3</sub>), 4.75 (s, 2H, H11), 6.90 (d, J = 8.7 Hz, 2H, aryl B), 7.11 (d, J = 8.8 Hz, 2H, aryl A), 7.25 (d, J = 8.7 Hz, 2H, aryl B), 7.60 (d, J = 8.9 Hz, 2H, aryl A), 7.91 (s, 1H, H7).

$^{13}C$ -NMR (100 MHz, DMSO-d<sub>6</sub>) δ 44.1 (CH<sub>2</sub>, C11), 55.1 (OCH<sub>3</sub>), 55.5 (OCH<sub>3</sub>), 114.0 (CH), 115.0 (CH), 117.8 (C), 125.4 (C), 129.4 (CH), 127.1 (C), 132.3 (CH), 133.4 (CH, C7), 158.9 (C), 161.3 (C), 165.6 (C=O), 167.3 (C=O).

**3-(4-fluorobenzyl)-5-(4-methoxybenzylidene)thiazolidine-2,4-dione; 4CI [23]**

$C_{18}H_{14}FNO_3S$ . Yield: 49 %. Mp: 127–130 °C.

MS (70 eV): m/z (%): 343 ( $M^+$ , 51), 164 (100), 109 (75), 149 (35).

**5-benzylidene-3-(3-chlorobenzyl)thiazolidine-2,4-dione; 4DF**

$C_{17}H_{12}ClNO_2S$ . Yield: 39%. Mp: 143–146 °C.

MS (70 eV): m/z (%): 329 ( $M^+$ , 24), 134 (100), 89 (15), 70 (6).

$^1H$ -NMR (600 MHz, DMSO-d<sub>6</sub>) δ 4.85 (s, 2H, H11), 7.28 (d, J = 7.0 Hz, 1H, aryl B), 7.37-7.40 (m, 3H, aryl B), 7.50 (t, J = 7.3 Hz, 1H, aryl A), 7.55 (t, J = 7.4 Hz, 2H, aryl A), 7.63 (d, J = 8.5 Hz, 2H, aryl A), 7.96 (s, 1H, H7).

$^{13}C$ -NMR (150 MHz, DMSO-d<sub>6</sub>) δ 44.0 (CH<sub>2</sub>, C11), 121.1 (C), 126.2 (CH, aryl B), 127.5 (CH, aryl B), 127.7 (CH, aryl B), 129.2 (2 CH, aryl A), 130.0 (2 CH, aryl A),

130.4 (CH, aryl B), 130.6 (CH, aryl A), 132.8 (C), 133.1 (C), 133.4 (CH, C7), 137.7 (C), 165.3 (C=O), 167.2 (C=O).

**5-benzylidene-3-(4-chlorobenzyl)thiazolidine-2,4-dione; 4DG [19]**

$C_{17}H_{12}ClNO_2S$ . Yield: 27 %. Mp: 159–162 °C.

MS (70 eV): m/z (%): 329 ( $M^+$ , 35), 134 (100), 125 (88), 89 (25).

**5-benzylidene-3-(4-methoxybenzyl)thiazolidine-2,4-dione; 4DH**

$C_{18}H_{15}NO_3S$ . Yield: 13%. Mp: 128–131 °C

MS (70 eV): m/z (%): 325 ( $M^+$ , 10), 121 (100), 134 (10), 77 (8).

$^1H$ -NMR (600 MHz, DMSO-d<sub>6</sub>) δ 7.93 (s, 1H, H7), 3.71 (s, 3H, OCH<sub>3</sub>), 4.75 (s, 2H, H11), 6.90 (d, J = 8.7 Hz, 2H, aryl B), 7.25 (d, J = 8.7 Hz, 2H, aryl B), 7.49 (t, J = 7.3 Hz, 1H, aryl A), 7.53 (t, J = 7.4 Hz, 2H, aryl A), 7.61 (d, J = 7.3 Hz, 2H, aryl A).

$^{13}C$ -NMR (150 MHz, DMSO-d<sub>6</sub>) δ 44.3 (CH<sub>2</sub>, C11), 55.2 (OCH<sub>3</sub>, C18), 114.1 (2CH, aryl B), 121.2 (C), 127.5 (C), 129.4 (2CH, aryl A), 129.5 (2CH, aryl B), 130.2 (2 CH, aryl A), 130.8 (CH, aryl A), 132.9 (C), 133.4 (CH, C7), 159.0 (C), 165.5 (C=O), 167.3 (C=O).

**5-benzylidene-3-(4-fluorobenzyl)thiazolidine-2,4-dione; 4DI [24]**

$C_{17}H_{12}FNO_2S$ . Yield: 33 %. Mp: 129–132 °C.

MS (70 eV): m/z (%): 313 ( $M^+$ , 38), 109 (100), 134 (65), 83 (10).

**5-(4-bromobenzylidene)-3-(4-methoxybenzyl) thiazolidine-2,4-dione; 4EH**

$C_{18}H_{14}BrNO_3S$ . Yield: 23%. Mp: 169–172 °C

MS (70 eV): m/z (%): 403 ( $M^+$ , 5), 121 (100), 89 (6).

$^1H$ -NMR (400 MHz, DMSO-d<sub>6</sub>) δ 3.72 (s, 3H, OCH<sub>3</sub>), 4.76 (s, 2H, H11), 6.90 (d, J = 8.6 Hz, 2H, aryl B), 7.26 (d, J = 8.5 Hz, 2H, aryl B), 7.57 (d, J = 8.4 Hz, 2H, aryl A), 7.75 (d, J = 8.4 Hz, 2H, aryl A), 7.93 (s, 1H, H7).

<sup>13</sup>C-NMR (100 MHz, DMSO-d<sub>6</sub>) δ 44.8 (CH<sub>2</sub>, C11), 55.6 (OCH<sub>3</sub>, C18), 114.5 (CH), 122.5 (C), 124.7 (C), 127.9 (C), 132.4 (CH), 129.9 (CH), 132.5 (C), 132.6 (C7), 132.9 (CH), 159.4 (C), 165.9 (C=O), 167.5 (C=O).

### 3.2 Cytotoxicity

Firstly, the cell viability of primary astrocyte cultures of rats against TZDs **4AF-I** - **4DF-I** and **4EH** was evaluated. Cells were treated with compounds at a concentration of 100 μM for 72 h, and then cell viability was verified by the MTT assay. No significant differences were observed compared with the control, demonstrating that TZDs were not cytotoxic in astrocyte cells (**Figure 3**).

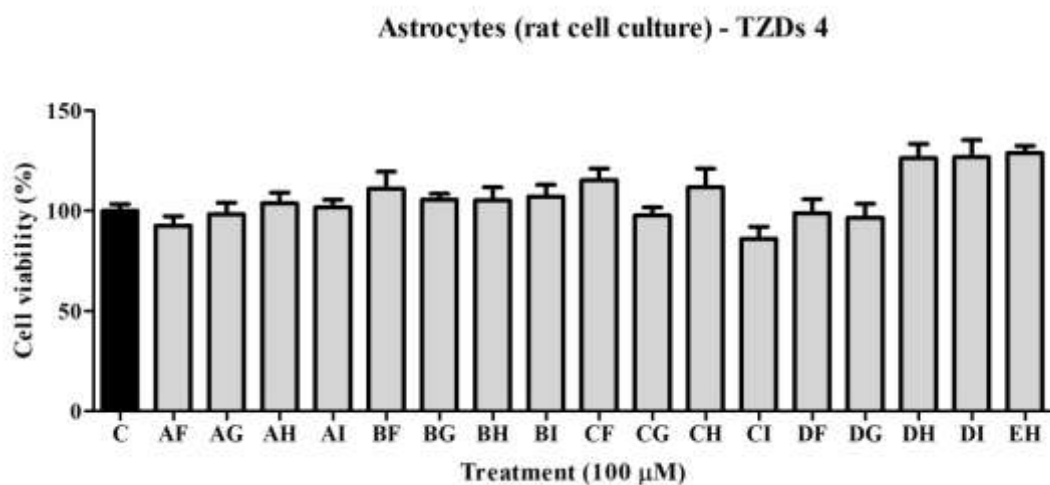


**Figure 3.** Effect of thiazolidinediones on primary astrocyte cultures of rats. Values are expressed as mean ± standard error from at least three independent experiments performed in triplicate. Data were analyzed using one-way analysis of variance (ANOVA) and Tukey's test.

Then, we determine the cytotoxicity of the synthesized compounds in mouse (GL261) and rat (C6) glioblastoma cell lines. All compounds were significantly more cytotoxic than the control DMSO, except for **4CG** and **4CH** in mouse cell lines GL261 (**Figure 4A**). These compounds have the same group R<sup>1</sup> = 4-OCH<sub>3</sub>, and R<sup>2</sup> = 4-Cl for compound **4CG** and R<sup>2</sup> = 4-OCH<sub>3</sub> for **4CH**. The presence of the same groups in both rings reduces the antitumor activity in mouse cell lines (**4AG**, **4BI**, **4CH**).

In rat glioma cell lines C6, all TZDs showed significant statistical difference at 100  $\mu$ M, and the best results were found for compounds **4CI** and **4DI** (**Figure 4B**). These two compounds have the fluorine atom at the *para* position of ring B.

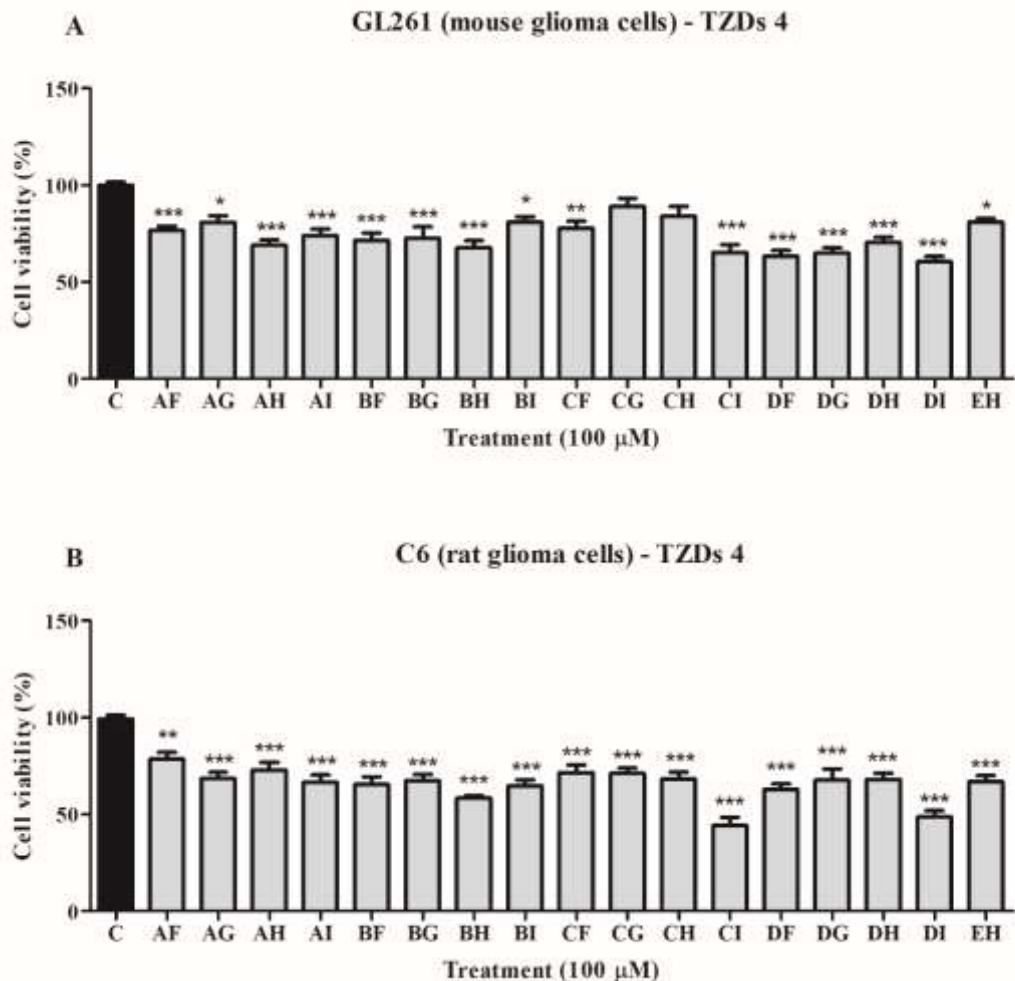


**Figure 4.** (A) Antitumor effect of TZDs on GL261 mice glioblastoma cells. (B) Antitumor effect of TZDs on C6 rat glioblastoma cells. Values are expressed as mean  $\pm$  standard error from at least three independent experiments performed in triplicate. Data were analyzed using one-way analysis of variance (ANOVA) and Tukey's test. Differences between the mean values were considered significant when  $*P < 0.05$ ,  $**P < 0.01$ , and  $***P < 0.001$ .

Therefore, compounds **4CI** and **4DI** were selected for testing at 25, 50, 100, 175, and 250  $\mu\text{M}$  concentrations in the C6 rat cell line assay. Their IC<sub>50</sub> values were 28.51  $\mu\text{M}$  and 54.26  $\mu\text{M}$ , respectively (**Figure 5**).

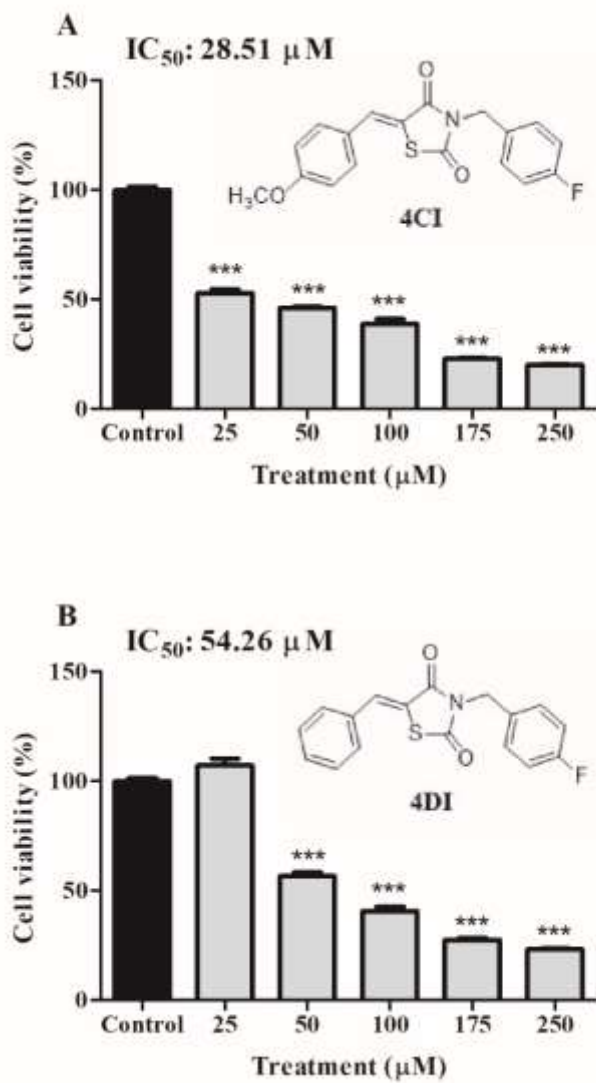


**Figure 5.** Antitumor effect of compound (A) **4CI** and (B) **4DI** on C6 rat glioblastoma cells. Values were expressed as mean  $\pm$  standard error from at least three independent experiments performed in triplicate. Data were analyzed using a one-way analysis of variance and Tukey's test. Differences between the mean values were considered significant when \* $P < 0.05$ , \*\* $P < 0.01$ , and \*\*\*  $P < 0.001$ .

Recently, we studied some thiazolidinones against glioma C6 and found that the 72 hours is important for anti-glioma activity. Those compounds also showed selectivity to glioma cells once no cytotoxic activity in astrocytes was observed at same concentration of 100  $\mu$ M [25].

The study performed by Metwally et al. [8b] revealed that 5-(4-methoxybenzylidene)-3-[(3-phenyl-3,4-dihydro-4-oxoquinazolin-2yl)methyl]thiazolidine-2,4-dione was cytotoxic in three cell lines: PC-3 (prostate adenocarcinoma), MDA-MB-231 (breast adenocarcinoma), and HT-1080 (fibrosarcoma), with IC<sub>50</sub> values of 79.6  $\mu$ M, 32  $\mu$ M, and 47.8  $\mu$ M, respectively. The said compound and **4CI** have a methoxy substituent at the *para* position of the benzylidene ring (ring A), demonstrating that this group at this position may be important for antitumor activity in different cell lines.

In the study by Rego *et al.* [8c], the cytotoxicities of three structures against human glioblastoma cell lines (NG97) were analyzed. The compounds have 4-NO<sub>2</sub> and 3-Br (LPSF/SF-13) substituents on ring B and 3-Br, 4-OCH<sub>3</sub> (LPSF/SF-15), and 3,4,5-OCH<sub>3</sub> (LPSF/SF-17 R) substituents on ring A. The presence of the 3-Br group on ring A may have contributed to its cytotoxicity against the lineage NG97 because the best results were obtained for the molecule LPSF/SF-13 (IC<sub>50</sub> of 73.73  $\mu$ M) in the MTT assay. Although the glioblastoma cell line used in our study is different, the results we found were better (IC<sub>50</sub> = 28  $\mu$ M) than that of Rego *et. al.* (IC<sub>50</sub> = 73.73  $\mu$ M), demonstrating that the presence of only one 4-OMe group can be important for antitumor activity. In addition, Rego *et al.* [8c] found, through molecular modeling study, that the 4-NO<sub>2</sub> substituent on ring B is capable of hydrogen bonding with the PPAR $\gamma$  receptor, which may be related to the antitumor activity of TZDs. Similar to LPSF/SF-13R, the structures of **4CI** and **4DI** have a substituent capable of hydrogen bonding on ring B (4-F). Additionally, changes in ring B substituents can significantly alter the cytotoxicity in mouse (GL261) and rat (C6) glioblastoma cell lines; therefore, the presence of both 4-OMe in ring A and 4-F in ring B appears to contribute to anti-glioma activity.

Both rosiglitazone and pioglitazone have structural differences, such as the benzyl ring instead of benzylidene and the substituents attached to ring A. However, they are also similar in the -OR substituents in the *para* position of ring A, specifically at the pioglitazone R=2,5-diethylpyridine, and rosiglitazone R=N-ethyl-N-methylpyridin-2-

amine. This contributes to the knowledge that substituents at this position are associated with antitumor activity.

Accordingly, the presence of only one OR substituent at the *para*-position of ring and substituents that can perform hydrogen bonding at the *para*-position of ring B appear to contribute to the antitumor activity of TZDs. The exact mechanism of antitumor action of glitazones is yet to be understood. We speculate that it occurs via PPAR $\gamma$ , and thus, structures capable of activating this receptor are promising. Pre-clinical and clinical studies have obtained satisfactory results regarding the antitumor activity of TZDs. However, only a few studies have correlated structure and the anti-glioma activity. Therefore, further studies are needed to better understand this relationship, allowing the design of structures with greater effectiveness and safety.

#### **4. CONCLUSION**

The seventeen compounds were significantly more cytotoxic with respect to the control in the glioblastoma C6 cell line, and most of these TZDs were also cytotoxic in the GL261 cell line. The compounds were not cytotoxic in astrocyte culture, demonstrating selectivity for malignant cells. Presumably, changes in both rings are important for anti-glioma activity in the cell lines tested. The structure **4CI**, which has a fluorine atom at position 4 of ring B and a methoxy at position 4 of ring A, obtained the best result with an IC<sub>50</sub> value of 28.51  $\mu$ M. This compound is recommended to be studied in future *in vivo* experiments as a continuation of our research program.

#### **ETHICS APPROVAL AND CONSENT TO PARTICIPATE**

All procedures used in the present study followed the “Principles of Laboratory Animal Care” of the National Institutes of Health (NIH) and were approved by the Ethical Committee of UFPel (CEEA 9219).

#### **AVAILABILITY OF DATA AND MATERIALS**

The data that support the findings of this study are available from the corresponding author, [WC], upon reasonable request.

## **FUNDING**

Fundação de Amparo à Pesquisa do Rio Grande do Sul (FAPERGS - 17/2551-0000988-6) and Coordenação de Aperfeiçoamento de Pessoal de Nível Superior- Brasil (CAPES) – Finance code 001

## **CONFLICT OF INTEREST**

The authors declare no conflict of interest.

## **ACKNOWLEDGEMENTS**

W. C. is recipient of the CNPq fellowship. The authors also acknowledge the NUQUIMHE X-ray team (Department of Chemistry - UFSM), especially Anderson Pagliari, for the kindly collection and refinement of the data.

## **REFERENCES**

1. a) Ferlay, J.; Parkin, D.M.; Steliarova-Foucher, E. Estimates of cancer incidence and mortality in Europe in 2006. *Eur. J. Cancer*, **2010**, *46*, 765-781. b) Ostrom, Q.T.; Gittleman, H.; Liao, P.; Rouse, C.; Chen, Y.; Dowling, J.; Wolinsky, Y.; Kruchko, C.; Barnholtz-Sloan, J. CBTRUS statistical report: primary brain and central nervous system tumors diagnosed in the united states in 2007–2011. *Neuro Oncol.*, **2014**, *16*, iv1–iv63.
2. Weller, M.; Wick, W.; Aldape, K.; Brada, M.; Berger, M.; Pfister, S.M.; Nishikawa, R.; Rosenthal, M.; Wen, P.Y.; Stupp, R.; Reifenberger, G. Glioma. *Nat. Rev. Dis. Primers*, **2015**, *1*, 15017. <https://doi.org/10.1038/nrdp.2015.17>.
3. Ohgaki, H.; Kleihues, P. Epidemiology and etiology of gliomas. *Acta Neuropathol.*, **2005**, *109*, 93-108.
4. Napoleon, A.A. Review on recent developments and biological activities of 2,4-thiazolidinediones. *Int. J. PharmTech Res.*, **2016**, *9*, 429-443.
5. Radi, M.; Botta, L.; Casaluce, G.; Bernardini, M.; Botta, M. Practical *one-pot* two-step protocol for the microwave-assisted synthesis of highly functionalized rhodanine derivatives. *Comb. Chem.*, **2010**, *12*, 200-205.

6. Naim, M.J.; Alam, M.J.; Ahmad, S; Nawaz, F; Shrivastava, N; Sahu, M; Alam, O. Therapeutic journey of 2,4-thiazolidinediones as a versatile scaffold: An insight into structure activity relationship. *Eur. J. Med. Chem.*, **2017**, *129*, 218-250.
7. a) Chinthala, Y.; Domatti, A.K.; Sarfaraz, A.; Singh, S.P.; Arigari, N.K.; Gupta, N.; Satya, S.K.V.N.; Kumar, J.K.; Khan, F.; Tiwari, A.K.; Paramjit, G. Synthesis, biological evaluation and molecular modeling studies of some novel thiazolidinediones with triazole ring. *Eur. J. Med. Chem.*, **2013**, *70*, 308-314. b) Flament, S.; Martin, H.; Richert, L.; Chapleur, Y.; Boisbrun, M. Synthesis of new troglitazone derivatives: Anti-proliferative activity in breast cancer cell lines and preliminary toxicological study. *Eur. J. Med. Chem.*, **2012**, *51*, 206-215.
8. a) Fröhlich, E.; Wahl, R. Chemotherapy and chemoprevention by thiazolidinediones. *BioMed. Res. Int.*, **2015**, *2015*, 845340 article ID 845340 (14 pages). b) Metwally, K.; Pratsinis, H.; Kletsas, D. Novel 2,4-thiazolidinediones: Synthesis, in vitro cytotoxic activity and mechanistic investigation. *Eur. J. Med. Chem.*, **2017**, *133*, 340-350. c) Rêgo, M.J.B.M.; Galdino-Pitta, M.R.; Pereira, D.T.M.; Silva, J.C.; Rabello, M.M.; Lima, M.C.A.; Hernandes, M.Z.; Pitta, I.R.; Galdino, S.L.; Pitta, M.G.R. Synthesis, in vitro anticancer activity and in silico study of new disubstituted thiazolidinedione derivatives. *Med. Chem. Res.*, **2014**, *23*, 3220-3226.
9. Hau, P.; Kunz-Schughart, L.; Bogdahn, U.; Baumgart, U.; Hirschmann, B.; Weimann, E.; Muhleisen, H.; Ruemmele, P.; Steinbrecher, A.; Reichle, A. Low-dose chemotherapy in combination with COX-2 inhibitors and PPAR-gamma agonists in recurrent high-grade gliomas - a phase II study, *Oncology*, **2007**, *73*, 21-25.
10. Sheldrick, G.M. A short history of SHELX. *Acta Crystallogr. Sect. A*, **2008**, *64*, 112-122.
11. Farrugia, L.J. WinGX and ORTEP for Windows: An Update. *J. Appl. Crystallogr.*, **2012**, *45*, 849-854.
12. Da Frota Junior, M.L.J.; Braganhol, E.; Canedo, A.D.; Klamt, F.; Apel, M.A.; Mothes, B.; Lerner, C.; Battastini, A.M.O.; Henriques, A.T.; Moreira, J.C.F.

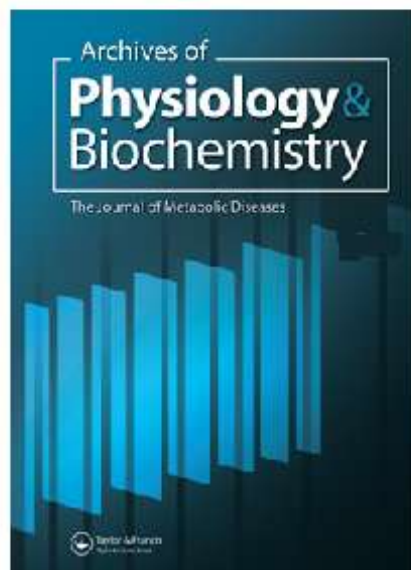
- Brazilian marine sponge *Polymastia janeirensis* induces apoptotic cell death in human U138MG glioma cell line, but not in a normal cell culture. *Invest. New Drugs*, **2009**, *27*, 13-20.
13. Mosmann, T. Rapid colorimetric assay for cellular growth and survival: application to proliferation and cytotoxicity assays. *J. Immunol. Methods*, **1983**, *65*, 55–63.
14. Drawanz, B.B.; Ribeiro, C.S.; Masteloto, H.G.; Neuenfeldt, P.D.; Pereira, C.M.P.; Siqueira, G.M.; Cunico, W. Sonochemistry: a good, fast and clean method to promote the synthesis of 5-arylidene-2,4-thiazolidinediones. *Ultrason. Sonochem.*, **2014**, *21*, 1615-1617.
15. Alegaon, S.G.; Alagawadi, K.R. New thiazolidine-2,4-diones as antimicrobial and cytotoxic agent. *Med. Chem. Res.*, **2012**, *21*, 3214-3223.
16. Pitta, I.R.; Bosso, C.; Goes, A.J.S.; Lima, M.C.A.; Galdino, S.L.; Cuong, L. Mass spectrometry of some benzylidene imidazolidinediones and thiazolidinediones. III. Positive and negative electron impact mass spectra of chlorobenzyl imidazolidinedione or thiazolidinedione compounds. *Spectrosc. Lett.*, **1992**, *23*, 419-431.
17. Goes, A.J.S.; de Lima, M.C.A.; Galdino, S.L.; Pitta, I.R.; Luu-Duc, C. Synthesis and antimicrobial activity of fluorobenzyl (benzylidene) thiazolidinediones and substituted imidazolidinediones. *J. Pharm. Belg.*, **1991**, *46*, 236-240.
18. Barros, C.D.; Amato, A.A.; De Oliveira, T.B.; Iannini, K.B.R.; Da Silva, A.L.; Da Silva, T.G.; Leite, E.S.; Hernandes, M.Z.; De Lima, M.D.C.A.; Galdino, S.L.; Neves, F.D.A.R.; Pitta, I.R. Synthesis and anti-inflammatory activity of new arylidene-thiazolidine-2,4-diones as PPAR $\gamma$  ligands. *Bioorg. Med. Chem.*, **2010**, *18*, 3805-3811.
19. Malik, S.; Choudhary, A.; Kumar, S.; Bhola, A.; Kumar, A. Synthesis of some novel substituted-arylidene and substituted-benzylthiazolidine-2,4-dione analogues as chemotherapeutic agents. *Pharma Chemica*, **2010**, *2*, 17-21.
20. Galdino, S.L.; Lima, M.C.A.; Goes, A.J.S.; Pitta, I.R.; Duc, C.L. Mass spectrometry of some benzylidene imidazolidinediones and thiazolidinediones. II. Chlorobenzyl

- imidazolidinedione and fluoro or chlorobenzyl thiazolidinedione compounds. *Spectrosc. Lett.*, **1991**, 24, 1013-1021.
21. Albers, H.M.H.G.; Kuijl, C.; Bakker, J.; Hendrickx, L.; Wekker, S.; Farhou, N.; Liu, N.; Blasco-moreno, B.; Scanu, T.; Hertog, J.D.; Celie, P.; Ovaa, H.; Neefjes, J. Integrating chemical and genetic silencing strategies to identify host kinase-phosphatase inhibitor networks that control bacterial infection. *ACS Chem. Biol.*, **2014**, 9, 414–422.
22. a) Silva, D.S.; Silva, C.E.H.; Soares, M.S.P.; Azambuja, J.H.; Carvalho, T.R.; Zimmer, G.C.; Frizzo, C.P.; Braganhol, E.; Spanevello, R.M.; Cunico, W. Thiazolidin-4-ones from 4-(methylthio)benzaldehyde and 4-(methylsulfonyl)benzaldehyde: Synthesis, anti-glioma activity and cytotoxicity. *Eur. J. Med. Chem.*, **2016**, 124, 574-582. b) Silveira, E.F.; Azambuja, J.H.; Carvalho, T.R.; Kunzler, A.; Silva, D.S.; Teixeira, F.C.; Rodrigues, R.; Beira, F.T.; Alves, R.C.S.A.; Spanevello, R.M.; Cunico, W.; Stefanello, F.M.; Horn, A.P.; Braganhol, E. Synthetic 2-aryl-3-((piperidin-1-yl)ethyl)thiazolidin-4-ones exhibit selective in vitro antitumoral activity and inhibit cancer cell growth in a preclinical model of glioblastoma multiforme. *Chem. Biol. Interact.*, **2017**, 266, 1-9.
23. Wang, P.; Yu, J.; Yin, Q.; Li, W.; Ren, X.; Hao, X. Rosiglitazone Suppresses Glioma Cell Growth and Cell Cycle by Blocking the Transforming Growth Factor-Beta Mediated Pathway. *Neurochem. Res.*, **2012**, 37, 2076–2084.
24. a) Weng, J.; Chen, C.; Pinzone, J.; Ringel, M.; Chen, C. Beyond peroxisome proliferator-activated receptor gamma signaling: the multi-facets of the antitumor effect of thiazolidinediones. *Endocr. Relat. Cancer*, **2006**, 13, 401-413. b) Chou, F.; Wang, P.; Kulp, S.; Pinzone, J. Effects of thiazolidinediones on differentiation, proliferation, and apoptosis. *Mol. Cancer Res.*, **2007**, 5, 523-530. c) Liu, K.; Rao, W.; Parikh, H.; Li, Q.; Guo, T.; Grant, S.; Kellogg, G.; Zhang, S. 3,5-Disubstituted-thiazolidine-2,4-dione analogs as anticancer agents: design, synthesis and biological characterization, *Eur. J. Med. Chem.*, **2012**, 47, 125-137.
25. Grommes, C.; Karlo, J.C.; Caprariello, A.; Blankenship, D.; Dechant, A.; Landreth, G.E. The PPAR $\gamma$  agonist pioglitazone crosses the blood-brain barrier and reduces tumor growth in a human xenograft model, *Cancer Chemother. Pharmacol.*, **2013**, 71, 929-936.

## **4.2 MANUSCRITO**

O manuscrito foi submetido à revista Archives of Physiology and Biochemistry.

A aprovação junto ao comitê de ética em experimentação animal (CEEA) autorizando a realização da pesquisa desenvolvida neste manuscrito encontra-se em anexo a esta tese (**ANEXO A**). O comprovante de submissão pode ser conferido no **ANEXO C**.



**3-(4-fluorobenzyl)-5-(4-methoxybenzylidene)thiazolidine-2,4-dione exhibits antglioma effect and reverts behavioral and biochemical changes in an experimental model of glioma**

Journal:	<i>Archives Of Physiology And Biochemistry</i>
Manuscript ID	NAPB-2020-0396
Manuscript Type:	Original Paper
Date Submitted by the Author:	14-May-2020
Complete List of Authors:	Vasconcelos, Alana; Universidade Federal de Pelotas, CCQFA de Moura, Larissa; Universidade Federal de Pelotas, CCQFA Pedra, Nathalia ; Universidade Federal de Pelotas Bona, Natália; Universidade Federal de Pelotas Soares, Mayara; Universidade Federal de Pelotas Spohr, Luiza; Universidade Federal de Pelotas Spanevello, Roselia; Universidade Federal de Pelotas Barschak, Alethea; Universidade Federal de Ciencias da Saude de Porto Alegre Stefanello, Francieli; Universidade Federal de Pelotas, Cunico, Wilson; Universidade Federal de Pelotas, CCQFA
Keywords:	glioblastoma multiforme, thiazolidine-2,4-dione, behavioral parameters, toxicity

URL: <http://mc.manuscriptcentral.com/napb> Email: eckel@uni-duesseldorf.de

**3-(4-fluorobenzyl)-5-(4-methoxybenzylidene)thiazolidine-2,4-dione exhibits antitumoral effect and reverts behavioral and biochemical changes in an experimental model of glioblastoma**

Alana de Vasconcelos<sup>a</sup>; Larissa Ribeiro de Moura;<sup>a</sup> Nathalia Stark Pedra<sup>b</sup>; Natália Pontes Bona<sup>b</sup>; Mayara Sandrielly Pereira Soares<sup>b</sup>; Luiza Spohr<sup>b</sup>; Roselia Maria Spanevello<sup>b</sup>; Aletháa Gatto Barschak<sup>c</sup>; Francieli Moro Stefanello<sup>b</sup>; Wilson Cunico<sup>a\*</sup>

<sup>a</sup>Laboratório de Química Aplicada à Bioativos (LaQuiABio), Centro de Ciências Químicas, Farmacêuticas e de Alimentos, Universidade Federal de Pelotas, Pelotas, RS, Brazil.

<sup>b</sup>Laboratório de Neuroquímica, inflamação e Câncer (Neurocan), Centro de Ciências Químicas, Farmacêuticas e de Alimentos, Universidade Federal de Pelotas, Pelotas, RS, Brazil.

<sup>c</sup>Departamento de Ciências Básicas da Universidade Federal de Ciências da Saúde de Porto Alegre, Porto Alegre, RS, Brazil.

\*Address reprint requests to: Wilson Cunico, Universidade Federal de Pelotas, Campus Universitário s/n, CEP 96160-000, Capão do Leão, RS, Brazil. Phone: +55 53 3275-7358; E-mail: [wjcunico@yahoo.com.br](mailto:wjcunico@yahoo.com.br)

## **Abstract**

The aim of the present study was to evaluate the anti-glioma activity of 3-(4-fluorobenzyl)-5-(4-methoxybenzylidene)thiazolidine-2,4-dione (AV23) in a preclinical model of glioblastoma, as well as behavioral parameters and toxicological profile. The implantation of C6 cells in the left striatum of male Wistar rats was performed by stereotaxic surgery. After recovery, animals were treated with vehicle (canola oil) or AV23 (10 mg/kg/day) intragastrically for 15 days. It was found that AV23 reduced the density of tumoral cells in brain. Serum biochemical parameters such as triglycerides, cholesterol, HDL-cholesterol, LDL-cholesterol, albumin, aspartate aminotransferase, urea, creatinine and total proteins were not changed; however, there was a slight increase in alanine aminotransferase. The compound AV23 reverted the hypoglycemia and the reduction in body weight caused by glioblastoma. Additionally, AV23 was able to revert the reduction of locomotion caused by the tumor implantation. Therefore, the compound AV23 can be considered a promising candidate in the treatment of glioblastoma.

**Keywords:** glioblastoma; thiazolidine-2,4-dione; behavioral parameters; toxicity

## **1. Introduction**

Thiazolidinedione (TZD) is a five-membered heterocyclic ring with two carbonyls at positions 2 and 4 (Napoleon et al., 2016), which can be functionalized at positions 5 and 3 by aldolic condensation reaction and *N*-alkylation reaction, respectively (Radi et al., 2010), these two reactions allow obtaining a large number of 2,4-thiazolidinedione derivatives with various biological activities described in the literature, including: anticancer, anti-inflammatory, antidiabetic, antimicrobial, antiviral, antioxidant, neuroprotective, among others (Naim et al., 2017; Albers et al., 2014). These compounds can act as agonists of Peroxisome Proliferator-Activated Receptor Gamma (PPAR $\gamma$ ) (Yousefnia et al., 2018; Barros et al., 2010), whose activation seems to be important for the antiproliferative, antiangiogenic and apoptotic activity of these compounds, in different cancer cells (Yousefnia et al., 2018). The literature suggests that the antitumor action of TZDs is highly complex, involving a variety of genomic and non-genomic effects that can occur independently of PPAR $\gamma$  (Fröhlich and Wahl, 2015).

Synthetic TZD derivatives and medications, such as pioglitazone and ciglitazone (Lee et al., 2012; Rêgo et al., 2014; Fröhlich and Wahl, 2015; Ching et al. 2015; Yousefnia et al., 2018), have activity anti-glioma *in vitro*. Ching et al. 2015 found that pioglitazone has antiproliferative action by increasing the expression of EAAT2 glutamate transporters in U87MG glioblastoma cells, the increase in EAAT2 leads to a reduction in extracellular glutamate, which is important for the antiproliferative action. Ciglitazone mediates cell apoptosis by reducing Akt activity and inducing loss of mitochondrial membrane potential in T98G glioma cells (Lee et al., 2012). The anti-glioma action of TZDs may or may not be related to PPAR $\gamma$  activation (Lee et al., 2012; Ching et al. 2015; Fröhlich and Wahl, 2015).

According to the above, TZD derivatives are potential drugs against glioblastoma. This tumor is the most aggressive and common type of glioma and, although there are many advanced therapies, the response of glioblastoma to radiotherapy and chemotherapy is limited, leading to poor prognosis and low survival (about 13 to 15 months). Temozolomide (TMZ), a representative anti-cancer drug in the treatment of glioblastoma, increased the patient's average survival by only 2 months (Stupp et al., 2005). Other drugs, including some monoclonal antibodies, have been tested to establish new therapeutic protocols; however, no pharmacological intervention

has been shown to alter the course of the disease (Rhun et al., 2019).

Due to the low survival rate provided by the main medication used in glioblastoma therapy - TMZ, as well as the unsuccessful attempts to establish new protocols for this type of brain tumor (Rhun et al., 2019), synthesis and analysis are necessary the anti-glioblastoma activity of compounds from other pharmacological classes, including those derived from TZD, as these have already shown promising results as anti-glioblastoma agents (Ching et al., 2015; Yousefnia et al., 2018; Grommes et al., 2013; Hau et al., 2007; Rêgo et al., 2014).

In addition, compounds that have a central core similar to that of TZD have already demonstrated anti-glioblastoma activity *in vitro* and *in vivo*. In this context, our research group has studied the synthesis and anti-glioma activity of compounds containing the 4-thiazolidinone analogue (Silva, et al., 2016; Silveira, et al., 2017) and, recently, heterocycle TZD (Vasconcelos et al., 2020). Recently, we have demonstrated the anti-glioblastoma activity in C6 and GL261 cell lines of a synthetic series of TZDs, in which the compound 3- (4-fluorobenzyl) -5- (4-methoxybenzylidene) thiazolidine-2,4-dione stood out (**4CI, named AV23**), which obtained the  $IC_{50} = 28.51 \mu\text{M}$  in the MTT assay and did not affect normal astrocyte cell lines (Vasconcelos et al., 2020). Therefore, the present study focused on the assessment of anti-glioblastoma activity, toxicity and behavioral changes after treatment with **AV23** in a preclinical model of glioblastoma.

## 2. Materials and Methods

### 2.1. Animals

Thirty male Wistar rats with 60 days of age (250 - 300g) were kept under constant temperature, humidity and illumination, with food and water ad libitum. All experimental protocol was approved by the Animal Experimentation Ethics Committee on Animal Experimentation of institution, under protocol number CEEA 9219. The use of the animals is in accordance with the Brazilian Guidelines for the Care and Use of Research Animals in Sciences (DBCA) and according to the National Council for Animal Control and Experimentation (CONCEA)

## 2.2 Glioma implantation

For implantation of the glioma in the animals, C6 cells were grown under standard cell culture conditions. After reaching 90% confluence, C6 cells were resuspended in 3 µL of DMEM in a proportion of  $1 \times 10^6$ . Animals were previously anesthetized with ketamine and xylazine through intraperitoneal administration (i.p.) and later the animals underwent stereotactic surgery, where C6 cells were infused in the left striatum. Animals at a rate of 0.5 µL / min (coordinates with respect to bregma, 3.0 mm lateral, 0.5 later and 6 mm deep).

## 2.3. Treatment of animals

After surgery, the animals went through a 5-day recovery period. They were divided into 3 groups: (1) Sham (DMEM + Vehicle), (2) Control (Glioblastoma + Vehicle), (3) Treated (Glioblastoma + AV23 10 mg/kg/day dissolved in canola oil), and treated for 15 days intragastrically. The animals were weighed every 3 days and body weight gain was calculated. The animals were euthanized 21 days after the implantation of the tumor and had the brain and blood collected for further analysis (Figure 1A).

## 2.4. Behavioral Tests

### *2.4.1 Open Field Test*

The open field test measures the animals' ability to move around. The apparatus comprises a wooden box, which presents the floor divided into 16 equal quadrants. The animals are placed individually in the apparatus always in the same place, the number of times the animal crosses each quadrant during 5 min is counted (Walsh and Cummins 1976). The apparatus was cleaned with 40% ethanol before the entry of each animal.

### *2.4.2 Object Recognition*

After the open field test, the animals were subjected to the object recognition test using the same apparatus. The test aims to evaluate the animals' learning ability and short-term memory (Dere et al. 2005), based on the rodent's ability to investigate a new object. During the training phase, two identical objects in symmetrical positions are placed in the apparatus and the animals are free to explore for 5 min. After 3 hours, the test phase is carried out, where the animals are replaced in the apparatus with two

objects, one equal to the training phase (A), that is, a familiar object and a new object (B). Animals explore objects for 5 min, and exploration is understood when animals smell or touch objects such as nose and / or forelegs. The objects available have similar colors and textures, but differ in shape. An exploratory preference (%) is calculated using the ratio (TB X 100) / TA + TB. The apparatus and objects were cleaned with 40% ethanol before each animal entered.

## 2.5. Serum Biochemical Parameters

Blood was collected without anticoagulant and immediately centrifuged at 2500×g for 15 min. The clot was removed and the resulting serum was stored at – 80 °C for further biochemical determination. Hepatic and renal functions were evaluated using the following assays alanine aminotransferase (ALT), aspartate aminotransferase (AST), creatinine, urea, albumine and total proteins. Levels of glucose, tryglicerides, total cholesterol and fractions were also measured. These analyses were performed using a commercial kit (LABTEST, Diagnostica S.A., Minas Gerais, Brazil).

## 2.6. Statistical analysis

Data were expressed as means ± standard error. Statistical analyzes were performed using one-way analysis of variance (ANOVA) followed by Tukey's post hoc test. The differences were considered significant when associated with values of P<0.05.

## **3. Results**

To verify the anti-glioma potential of **AV23**, we performed tumor implantation in rats (Figure 1). According to Figure 1B, it was possible to observe that the animals treated with 10 mg/kg/day of **AV23** showed a reduction in tumoral density when compared to the control. As regards body weight (Figure 2), the compound **AV23** reverted the reduction of body weight gain induced by glioma implantation ( $F_{(2,18)} = 34.46$ ; P<0.001).

In addition, as shown in Table 1, there was a significant difference in glucose levels demonstrating a decrease in the levels of animals with glioblastoma when compared to sham and that treatment with **AV23** reduced this effect caused by glioma ( $F_{(2,15)} = 9.12$ ; P<0.01). We did not observe a significant difference in the levels of total

cholesterol, HDL, LDL, triglycerides, AST, urea, creatinine, albumin and total proteins ( $P>0.05$ ). However, there was a significant increase in ALT levels in animals treated with **AV23** ( $F_{(2,18)} = 13.80$ ;  $P<0.001$ ).

Figure 3 shows the effect of **AV23** treatment on behavioral parameters in the open field and object recognition tasks. In the open field test, it can be observed that the animals in the control group significantly decreased their locomotor activity when compared to the sham group, whereas **AV23** was able to revert this behavior ( $F_{(2,20)} = 18.20$ ;  $P<0.001$ ). We did not observe a significant difference in the numbers of groomings and rearings (data not shown) ( $P>0.05$ ). In object recognition task, we observed a reduction in the recognition index of a new object only in the control animals, demonstrating an alteration of short-term memory caused by glioma implantation ( $F_{(2,26)} = 4.88$ ;  $P<0.05$ ).

#### 4. Discussion

Considering the promising results obtained *in vitro* (Vasconcelos et al., 2020), in the present study we evaluated *in vivo* the anti-glioblastoma activity of 3-(4-fluorobenzyl)-5-(4-methoxybenzylidene)thiazolidine-2,4-dione (**AV23**), as well as the toxicological profile and behavioral parameters in rats. The **AV23** reduced the tumor volume qualitatively and normalized the glucose levels in the treated rats. There was no change in the lipid and protein profile, as well as in the serum markers of renal damage. AST levels did not change; however, there was an increase in ALT, both used to analyze liver damage. The **AV23** compound reverted the locomotor damage and the reduction of weight gain caused by glioblastoma.

In our previous study (Vasconcelos et al., 2020), the compound **AV23** obtained an  $IC_{50} = 28.51 \mu M$ , in the MTT assay, in C6 rat glioblastoma cell line. This value was lower than that found for the 5-(3-bromobenzylidene)-3-(4-nitrobenzyl) thiazolidine-2,4-dione (LPSF / SF-13), analyzed by the author Rêgo et al., 2014, which obtained an  $IC_{50}= 73.73 \mu M$ , in the glioblastoma cell line NG97. In addition, temozolamide, in C6 cell line, obtained an  $IC_{50}= 993.5 \mu M$  (Azambuja et al., 2018). These data demonstrate the great anti-glioblastoma potential of **AV23**.

The qualitative reduction in tumor volume after the administration of **AV23** in

the preclinical model of glioblastoma corroborates with the results found in the *in vitro* analysis and is in accordance with the findings of Grommes et al., 2013, who also found that derivatives of TZD have anti-glioblastoma activity *in vivo*. These authors demonstrated that pioglitazone reduces tumor volume in a model of glioma xenograft in mice. Pioglitazone was also effective in a phase II clinical study that evaluated the activity of pioglitazone and rofecoxib administered continuously, combined with chemotherapy (capecitabine or TMZ) in patients with high-grade gliomas (glioblastoma or anaplastic glioma) (Hau et al., 2007). Disease stabilization lasting more than three months was observed in 4 of 14 patients (29%). Thus, the study demonstrated that this regimen is moderately active and well tolerated in patients with high-grade glioma (Hau et al., 2007). This information demonstrates the importance of preclinical and clinical studies with different TZD derivatives, as well as the effectiveness of the tested compounds.

We also observed that **AV23** reverted the reduction in glucose levels caused by glioblastoma and normalized blood glucose levels. The reduction in blood glucose in control rats may be due to the Warburg effect (Figure 4), in which an excessive conversion of glucose into lactate occurs, even in the presence of sufficient oxygen, the effect is a metabolic characteristic of most cancer cells. Aerobic glycolysis, which generates about 32/30 moles of ATP per mole of glucose, is negatively regulated in cancer cells in favor of fermentation, which produces only two moles of ATP per mole of glucose, therefore, with the objective of producing a sufficient amount of ATP the tumor cells increase their glucose uptake (Movaheda et al., 2019). Since **AV23** reduced the number of viable C6 cells (Vasconcelos et al., 2020), there is a smaller number of tumor cells, therefore, less glucose uptake by the tumor, which probably results in the normalization of blood glucose levels in treated rats.

There was also a reversal of the reduction in weight gain caused by glioblastoma. These data can be explained by the fact that tumor cells can cause insulin resistance in normal cells (Yoshikawa et al., 1994; Klement, 2019), which would make glucose uptake in normal cells more difficult, leading to a reduction in weight gain in control rats and normalization in treated rats, due to the decreased viability of C6 cells caused by **AV23** (Vasconcelos et al., 2020).

The treatment also reverted the locomotor damage caused by glioblastoma. It is

possible to speculate that this effect is occurring due to some anti-inflammatory and / or analgesic action of **AV23**, since other TZD derivatives have already shown anti-inflammatory action in some studies (Barros et al., 2010; Wu et al., 2012; Unangst et al., 1994; Ali et al., 2007; Mckinnon et al. (2012). There was also an impairment of short-term memory in glioma-implanted rats and AV23 treatment was not able to restore this deficit.

There was no change in the lipid and protein profile of the treated rats, as well as no changes in the markers of renal damage after treatment. AST levels did not change; however, there was an increase in ALT, both enzymes used to verify liver damage. The alteration observed in ALT would not prevent new studies or even the commercialization of **AV23**, as some drugs, widely used in the clinic, such as, for example, valproic acid are able to alter ALT (Neves et al., 2006 ) in percentages much higher than those of **AV23**.

Based on the following findings: a) Tumor cells suffer the Warburg effect (Movaheda et al., 2019), that is, they need to capture more glucose. b) Several glucose transporters, including GLUT1, are positively regulated for the cell membrane of glioblastoma cells (Labak et al., 2016). c) The simultaneous presence of insulin and insulin-like growth factor (IGF-1) in astrocytes significantly increases the translocation of GLUT1 to the membrane (Fernandez et al., 2017). d) IGF-1 signaling is aberrant in several cancers (Pollak, 2012). e) Tumor cells can cause insulin resistance in normal cells (Yoshikawa et al., 1994; Klement, 2019). f) TZD analogs have been identified as potent inhibitors of IGF-1 receptors (Liu et al., 2010, Mughal et al., 2015). g) TZD analogs reduce insulin resistance and increase glucose uptake in normal cells (Bansal et al., 2020); figure 4 was prepared assuming a flow of glucose in the presence of glioblastoma cells and in the presence of TZDs + glioblastoma cells, an anti-tumor mechanism of action for **AV23** was also presumed - inhibition of the IGF-1 receptor.

## 5. Conclusion

The compound **AV23** was able to reduce tumor mass (qualitatively) in a preclinical model of glioblastoma. In addition, it reverted hypolocomotion and the reduction of glucose levels caused by tumor implantation. Serum analyzes performed after treatment with **AV23** in rats showed that the biochemical parameters of glucose, triglycerides,

cholesterol and kidney damage did not change; however, a slight increase in the enzyme ALT was observed.

Due to the low survival rate provided by the main drug used in glioblastoma therapy - TMZ (Stupp *et al.*, 2005), as well as the unsuccessful attempts to establish new protocols for this brain tumor (Rhun *et al.*, 2019), and studies demonstrating that TZD analogs have potential anti-glioblastoma action, it is important to investigate new molecules using preclinical and clinical studies. In this sense, complementary analyzes of **AV23** should be performed to include this compound in clinical studies.

### Acknowledgments

This study was financed by Fundação de Amparo à Pesquisa do Rio Grande do Sul (FAPERGS - 17/2551-0000988-6) and in part by the Coordenação de Aperfeiçoamento de Pessoal de Nível Superior - Brasil (CAPES) - Finance Code 001. W.C. and R.M.S. are recipient of the CNPq fellowship

### Conflict of interest

The authors declare that there are no conflicts of interest in this study.

### References

- Albers, H.M.H.G., *et al.*, 2014. Integrating chemical and genetic silencing strategies to identify host kinase-phosphatase inhibitor networks that control bacterial infection. *ACS Chem. Biol.*, 9, 414-422.
- Ali, A., *et al.*, 2007. Synthesis and three-dimensional qualitative structure selectivity relationship of 3, 5-disubstituted-2, 4-thiazolidinedione derivatives as COX2 inhibitors. *Arch. Pharm. Res.*, 30, 1186-1204.
- Azambuja, J.H., *et al.*, 2018. CD73 Downregulation decreases *in vitro* and *in vivo* glioblastoma growth. *Mol. Neurobiol.*, 56, 3260-3279.
- Bansal, G., *et al.*, 2020. An overview on medicinal perspective of thiazolidine-2,4-dione: A remarkable scaffold in the treatment of type 2 diabetes. *J Adv Res.*, 23, 163-205.

- Barros, C.D., *et al.*, 2010. Synthesis and anti-inflammatory activity of new arylidene-thiazolidine-2,4-diones as PPAR $\gamma$  ligands. *Bioorg. Med. Chem.*, 18, 3805-3811.
- Belzung, C. and Griebel, G., 2001. Measuring normal and pathological anxiety-like behaviour in mice: a review. *Behav Brain Res* 125, 141-149.
- Ching, J., *et al.*, 2015. The peroxisome proliferator activated receptor gamma agonist pioglitazone increases functional expression of the glutamate transporter excitatory amino acid transporter 2 (EAAT2) in human glioblastoma cells. *Oncotarget*, 6, 25, 21301-21314.
- Dere, E., *et al.*, 2005. Integrated memory for objects, places, and temporal order: Evidence for episodic-like memory in mice. *Neurobiol Learn Mem* 84, 214-221.
- Fernandez, A.M., *et al.*, 2017. Insulin regulates astrocytic glucose handling through cooperation with IGF-I. *Diabetes*, 66, 64-74.
- Fröhlich, E. and Wahl, R., 2015. Chemotherapy and Chemoprevention by Thiazolidinediones. Review Article. *Biomed Res. Int.*, 2015, ID 845340.
- Grommes, C., *et al.*, 2013. The PPAR $\gamma$  agonist pioglitazone crosses the blood-brain barrier and reduces tumor growth in a human xenograft model. *Cancer Chemother. Pharmacol.*, 71, 929-936.
- Hau, P., *et al.*, 2007. Low-dose chemotherapy in combination with COX-2 inhibitors and PPAR-gamma agonists in recurrent high-grade gliomas a phase II study. *Oncology*, 73, 21-25.
- Jin, Z., *et al.*, 2020. Structure of Mpro from COVID-19 virus and discovery of its inhibitors. *Nature*, <https://doi.org/10.1038/s41586-020-2223-y>.
- Klement, R.J., 2019. Wilhelm Brünings' forgotten contribution to the metabolic treatment of cancer utilizing hypoglycemia and a very low carbohydrate (ketogenic) diet. *J Tradit Complement Med*, 9, 192-200.
- Labak, C.M., *et al.*, 2016. Glucose transport: meeting the metabolic demands of cancer, and applications in glioblastoma treatment. *Am. J. Cancer Res.*, 6, 8, 1599-1608.

- Lee, M.W., *et al.*, 2012. Cell death is induced by ciglitazone, a peroxisome proliferator-activated receptor gamma (PPAR gamma) agonist, independently of PPAR gamma in human glioma cells. *Biochem Bioph Res Co*, 417, 552–557.
- Liu, X., *et al.*, 2010. Discovery and SAR of thiazolidine-2,4-dione analogues as insulin-like growth factor-1 receptor (IGF-1R) inhibitors via hierarchical virtual screening. *J.Med.Chem.*, 53, 2661-2665.
- McKinnon, B., *et al.*, 2012. Peroxisome proliferating activating receptor gamma-independent attenuation of interleukin 6 and interleukin 8 secretion from primary endometrial stromal cells by thiazolidinediones. *Fertil Steril*, 97, 3, 657-664.
- Movaheda, Z. G., *et al.*, 2019. Cancer cells change their glucose metabolism to overcome increased ROS: One step from cancer cell to cancer stem cell? *Biomed & Pharmacother.*, 112, 108690.
- Mughal, A., *et al.*, 2015. Effects of Thiazolidinediones on metabolism and cancer: Relative influence of PPAR $\gamma$  and IGF-1 signaling. *Eur. J. Pharmacol.*, 768, 217-225.
- Naim, M.J., *et al.*, 2017. Therapeutic journey of 2,4-thiazolidinediones as a versatile scaffold: An insight into structure activity relationship. *Eur. J. Med. Chem.*, 129, 218-250.
- Napoleon, A.A., *et al.*, 2016. Review on recent developments and biological activities of 2,4-thiazolidinediones. *Int. J. Pharm. Tech. Res.*, 9, 3, 429- 443.
- Neves, M.C., *et al.*, 2006. Hepatotoxicidade grave secundária a psicofármacos e indicação de eletroconvulsoterapia a paciente com esquizofrenia severe psychotropic-induced hepatotoxicity and indication of electroconvulsive therapy in a patient with schizophrenia. *J Bras Psiquiatr*, 55, 1, 74-77.
- Pollak, M., 2012. The insulin and insulin-like growth factor receptor family in neoplasia: an update. *Nat. Rev. Cancer*, 12 ,159–169.
- Radi, M., *et al.*, 2010. Practical *one-pot* two-step protocol for the microwave-assisted synthesis of highly functionalized rhodanine derivatives. *Comb. Chem.*, 12, 200-205.

- Rêgo, M.J.B.M., *et al.*, 2014. Synthesis, *in vitro* anticancer activity and in silico study of new disubstituted thiazolidinedione derivatives. *Med. Chem. Res.*, 23, 3220-3226.
- Rhun, E.L., *et al.*, 2019. Molecular targeted therapy of glioblastoma. *Cancer Treat. Rev.*, 80, ID 101896.
- Silva, D.S., *et al.*, 2016. Thiazolidin-4-ones from 4-(methylthio)benzaldehyde and 4-(methylsulfonyl)benzaldehyde: Synthesis, anti-glioma activity and cytotoxicity. *Eur. J. Med. Chem.*, 124, 574-582.
- Silveira, E.F., *et al.*, 2017. Synthetic 2-aryl-3-((piperidin-1-yl)ethyl)thiazolidin-4-ones exhibit selective in vitro antitumoral activity and inhibit cancer cell growth in a preclinical model of glioblastoma multiforme. *Chem-Biol Interact*, 266, 1-9.
- Stupp, R., *et al.*, 2005. Radiotherapy plus concomitant and adjuvant temozolomide for glioblastoma. *N. Engl. J. Med.*, 352, 987- 996.
- Unangst, P.C., *et al.*, 1994. Synthesis and biological evaluation of 5, 4[ 3, 5-bis(1,1-dimethylethyl) 4 hydroxyphenyl]methylene] oxazoles,-thiazoles, and -imidazoles: novel dual 5-lipoxygenase and cyclooxygenase inhibitors with antiinflammatory activity. *J. Med. Chem.*, 37, 322-328.
- Vasconcelos, A. *et al.*, 2020. 2,4-Thiazolidinedione as precursor to the synthesis of compounds with anti-glioma activities in C6 and GL261 cells. *Med. Chem.*, <https://doi.org/10.2174/1573406416666200403075826>.
- Walsh, R.N. and Cummins, R.A., 1976. The open-field test: a critical review. *Psychol Bull*, 83, 482-504.
- Wu, Y., *et al.*, 2012. Dynamic modeling of human 5-lipoxygenase-inhibitor interactions helps to discover novel inhibitors. *J. Med. Chem.*, 55, 2597–2605.
- Yoshikawa, T., *et al.*, 1994. Effects of tumor removal and body weight loss on insulin resistance in patients with cancer. *Surgery*, 116, 1, 62-66.
- Yousefnia, S., *et al.*, 2018. The influence of peroxisome proliferator-activated receptor  $\gamma$  (PPAR $\gamma$ ) ligands on cancer cell tumorigenicity. Review. *Gene*, 649, 14-22.

**Table 1.** Serum biochemical parameters in sham, glioma-implanted rats and treated with **AV23a**

	<b>Sham</b>	<b>Control</b>	<b>AV23</b>
Glucose (mg/dL)	114.8±4.81	89.8±7.99**	107.5±4.76##
Cholesterol (mg/dL)	70.2±8.38	69.0±3.76	79.2±4.54
HDL (mg/dL)	28.6±1.40	25.2±1.30	33.0±3.25
LDL (mg/dL)	27.6±7.47	30.7±3.31	31.4±2.70
Triglycerides (mg/dL)	71.0±6.69	69.2±2.79	80.3±8.22
ALT (U/L)	53.2±4.46	50.9±3.87**	76.7±3.21##
AST (U/L)	192.2±23.73	237.8±7.86	205.9±23.04
Urea (mg/dL)	47.2±3.06	51.2±4.35	50.3±2.33
Creatinine (mg/dL)	0.5±0.04	0.5±0.03	0.4±0.03
Albumine (g/dL)	3.4±0.11	3.3±0.09	3.5±0.17
Total Proteins (g/dL)	6.2±0.19	6.0±0.17	6.6±0.29

<sup>a</sup> After the rats recovery period, they were divided into three groups: sham, control and **AV23** for 15 days. Values are the means ± standard errors (5-10 animals per group). The data were analyzed by one-way ANOVA followed by the Tukey test. \*\*P<0.01 when compared to the sham group. ##P<0.01 when compared to the control group.

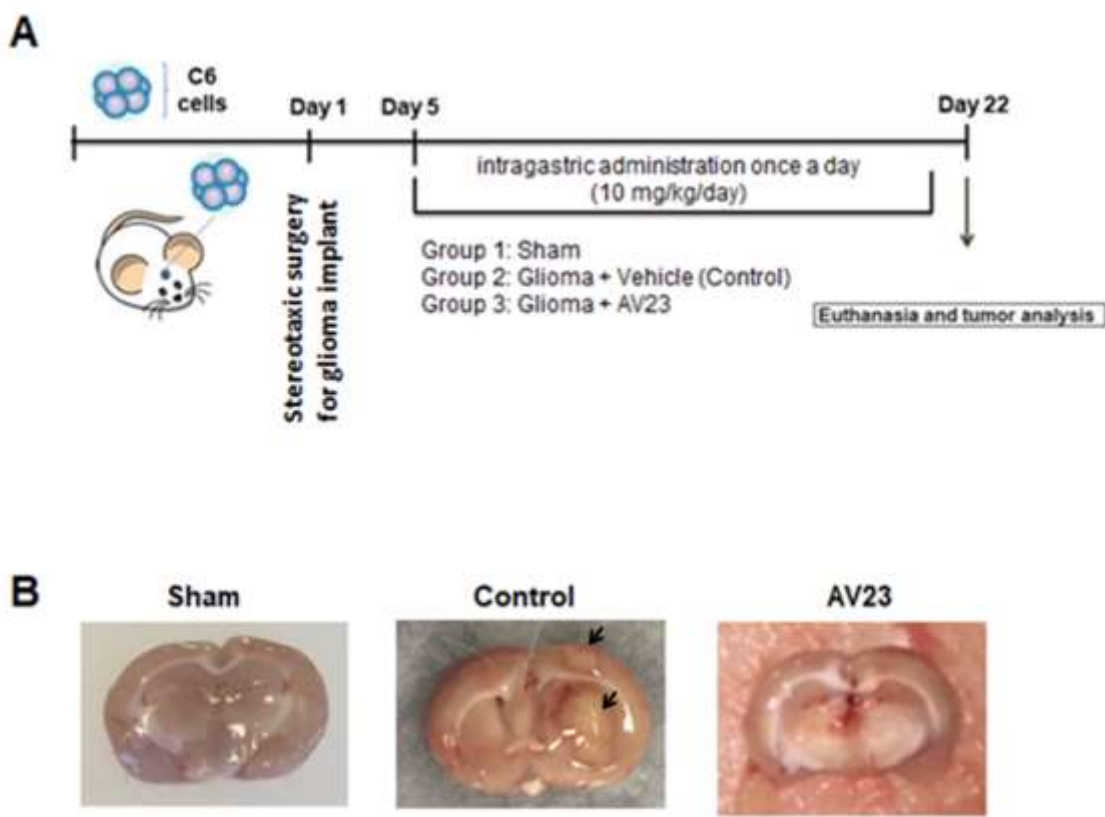


**Figure 1.** (A) C6 glioma cells were implanted intracerebroventricularly in adult rats and treatment was started 5 days later and was given for 15 days. On the 22nd day the animals were euthanized and the brain was collected. (B) Picture of some of the brains used for the qualitative assessment of tumor volume reduction.

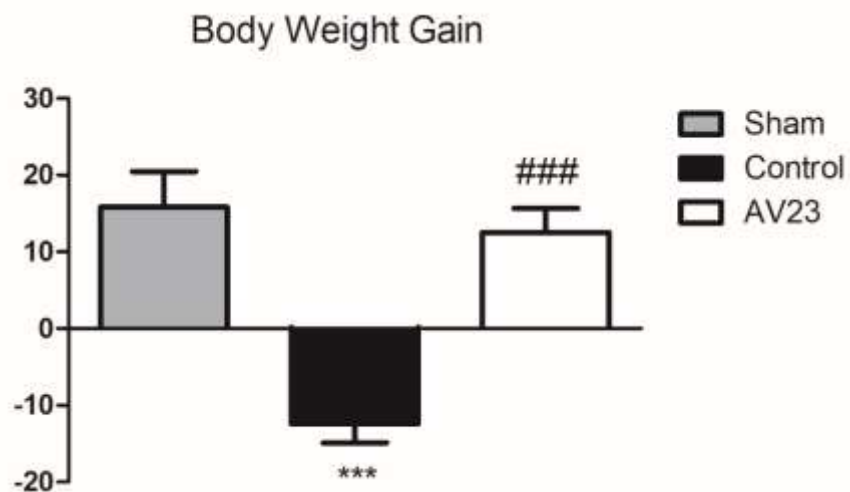


**Figure 2.** Body weight gain in sham, glioma-implanted rats and treated with **AV23**. Values represent the mean  $\pm$  SEM ( $n = 7$  animals per group). Data were analyzed by one-way ANOVA followed by post-hoc comparisons (Tukey's test). \*\*\* $P < 0.001$  when compared with the sham group. ### $P < 0.001$  when compared with the control group.

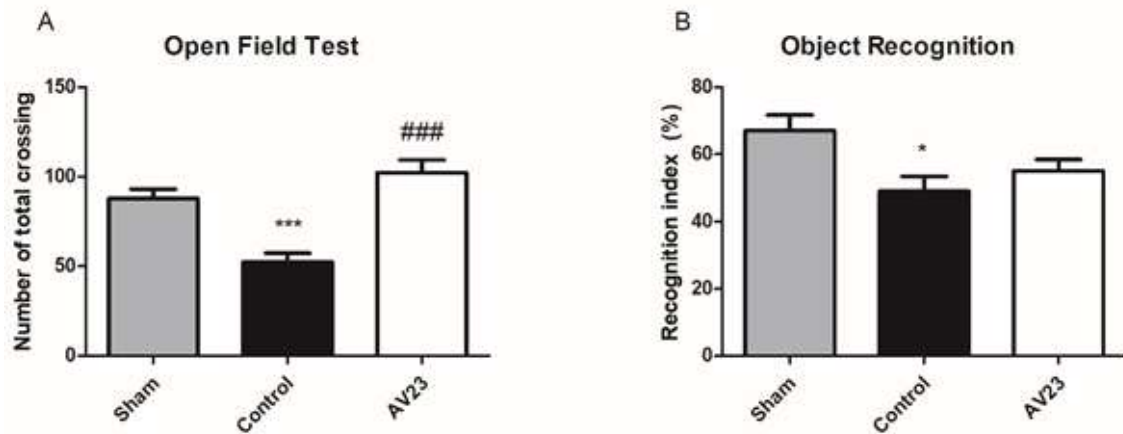


**Figure 3.** Effect of treatment with **AV23** (10 mg/kg/day) in glioma-implanted rats on behavioral parameters. The evaluation of locomotor activity was performed in the open field test (A). Short-term memory was determined using the object recognition test (B). Values are the means  $\pm$  standard errors ( $n = 7 - 10$  animals per group). Data were analyzed by one-way ANOVA followed by the Tukey test. \* $P < 0.05$  when compared with the sham group. \*\* $P < 0.001$  when compared with the sham group. #### $P < 0.001$  when compared with the control group.

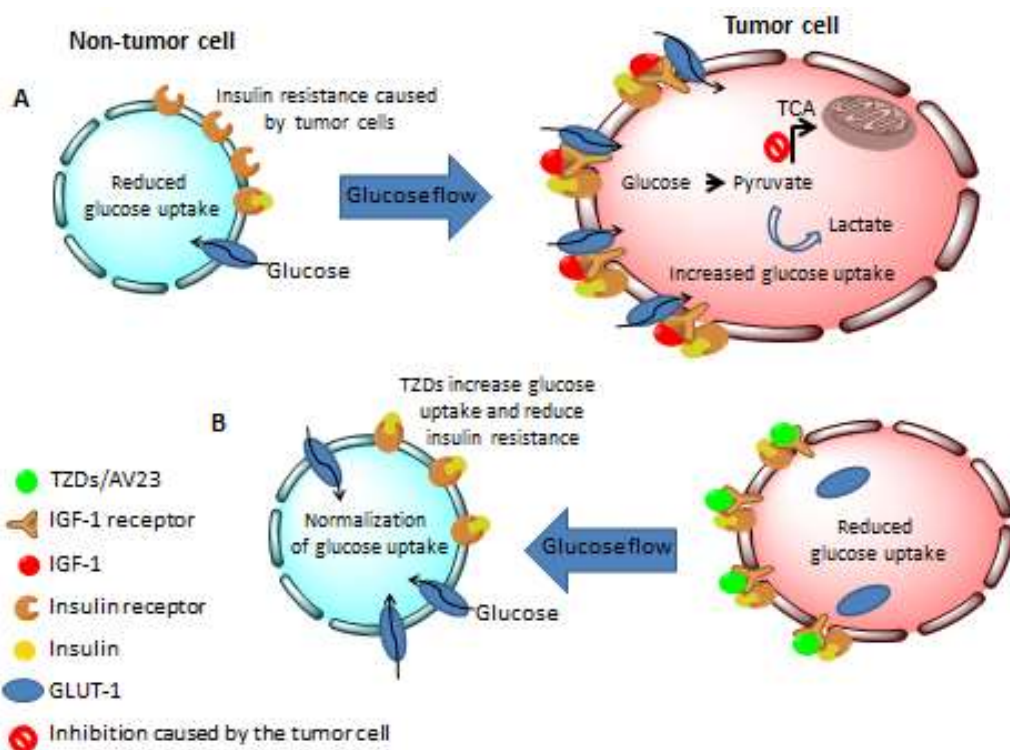


**Figure 4.** (A) Activation of IGF-1 and insulin receptors simultaneously and obtaining GLUT-1 translocation to the membrane, Warburg effect, increased glucose uptake in tumor cells and resistance to insulin caused by tumor cells. (B) Inhibition of the IGF-1 receptor by **AV23** and consequent reduction in the uptake of glucose in tumor cells, reduction of insulin resistance and increase in uptake of glucose caused by the **AV23** reversal of glucose flow.

## 5. CONCLUSÃO

Diante dos objetivos propostos para essa Tese, foi possível sintetizar e caracterizar 17 derivados de tiazolidinedionas com rendimentos de 12 a 49%. A metodologia de síntese *one-pot* em micro-ondas reduziu o tempo de reação comparado com a metodologia utilizada atualmente no laboratório. A purificação foi realizada utilizando reagentes não tóxicos o que contribui com uma química verde. Os resultados do CG-EM e do RMN de  $^1\text{H}$  e  $^{13}\text{C}$  comprovaram a formação correta das estruturas.

Os resultados *in vitro* demonstraram que todos os compostos foram citotóxicos na linhagem celular de glioblastoma de rato (C6) e que 15 TZDs reduziram a viabilidade celular na linhagem celular de glioblastoma de camundongo (GL261). Nenhum dos compostos foi citotóxico no cultivo primário de astrócitos, demonstrando seletividade para as células tumorais. Os melhores resultados foram obtidos para as estruturas **4Cl** ( $\text{IC}_{50}$  28,51  $\mu\text{M}$ ) e **4DI** ( $\text{IC}_{50}$  54,26  $\mu\text{M}$ ), as quais possuem  $R^2 = 4\text{F}$ , portanto, a presença do átomo de flúor na posição para do anel B parece ser importante para a ação antiglioblastoma dessa classe de compostos.

Nos testes posteriores verificou-se que o composto 3-(4-fluorobenzil)-5-(4-metoxibenzilideno)tiazolidina-2,4-diona **4Cl**: reduziu qualitativamente a massa tumoral dos ratos Wistar no modelo pré-clínico de glioblastoma multiforme; não alterou os seguintes parâmetros bioquímicos séricos nos ratos tratados: AST, HDL, LDL, colesterol total, triglicerídeos, proteínas totais, albumina, ureia e creatinina); aumentou os índices sorológicos da enzima ALT; reverteu o dano locomotor, a redução do ganho de peso e a redução da glicemia causados pelo glioblastoma.

O composto **4Cl**, portanto, possui atividade antiglioblastoma *in vivo* e o resultado obtido na ALT não impedirá a sua comercialização caso a atividade antiglioblastoma em humanos seja significativa e haja um aumento na sobrevida global dos pacientes. É importante mencionar que medicamentos capazes de alterar a ALT, em porcentagens bem maiores que o composto **4Cl**, são amplamente comercializados, como, por exemplo, o ácido valpróico.

A reversão do dano locomotor causada pelo composto **4CI** é um indício de que esse apresenta alguma ação anti-inflamatória e/ou analgésica e as normalizações do peso corporal e da glicemia podem estar relacionadas à redução do número de células tumorais viáveis. Em conjunto esses resultados demonstram uma melhora no estado geral dos animais tratados.

Em conclusão, o composto **4CI** demonstrou ser um potencial candidato a fármaco para uso clínico contra o glioblastoma, uma vez que nos testes *in vitro* reduziu a viabilidade celular das células C6 de maneira seletiva e no tratamento monoterápico verificou-se uma redução da massa tumoral e uma melhora geral dos ratos tratados. Além disto, esse composto poderia ser explorado em estudos de associação com outros medicamentos citostáticos e/ou em estudos com protocolos terapêuticos já definidos, objetivando a melhora da qualidade de vida dos pacientes e/ou potencialização da ação antitumoral dos fármacos utilizados atualmente na terapia do glioblastoma.

## 6. REFERÊNCIAS

ATLAS, T.C.G. Comprehensive genomic characterization defines human glioblastoma genes and core pathways. **Nature**, v. 455, p.1061-1068, 2008.

BASERGA, R. et al. The IGF-1 receptor in cancer biology. **Int. J. Cancer**, v. 107, p. 873-877, 2003.

BRENNAN, C.W. et al. The somatic genomic landscape of glioblastoma. **Cell**, v. 155, p.462-477, 2013.

CECCARELLI, M. et al; TCGA Research Network. Molecular profiling reveals biologically discrete subsets and pathways of progression in diffuse glioma. **Cell**., v.164, n.3, p.550-563, 2016.

CHING, J. The peroxisome proliferator activated receptor gamma agonist pioglitazone increases functional expression of the glutamate transporter excitatory amino acid transporter 2 (EAAT2) in human glioblastoma cells. **Oncotarget**, v. 6, n. 25, 2015.

CHUNG, W.J. Inhibition of cystine uptake disrupts the growth of primary brain tumors. **J Neurosci**, v. 25, p. 7101-7110, 2005.

DE CARVALHO, D.D.; YOU, J.S.; JONES P.A. DNA methylation and cellular reprogramming. **Trends Cell Biol**., v.20, n.10, p.609-617, 2010.

FELSBERG, J. et al. Epidermal growth factor receptor variant III (EGFRvIII) positivity in EGFR-amplified glioblastomas: prognostic role and comparison between primary and recurrent tumors. **Clin Cancer Res**, v.23, p. 6846-6855, 2017.

FERLAY, J. et al. Estimates of cancer incidence and mortality in Europe in 2006. **Eur. J. Cancer**, v. 46, p. 765-781, 2010.

FERRE, P. The biology of peroxisome proliferator-activated receptors: relationship with lipid metabolism and insulin sensitivity. **Diabetes**, v. 53, p. S43– S50, 2004.

FERNANDEZ, A.M. et al. Insulin regulates astrocytic glucose handling through cooperation with IGF-I. **Diabetes**, v. 66, p.64-74, 2017.

FRÖHLICH, E. and WAHL, R. Chemotherapy and Chemoprevention by Thiazolidinediones. Review Article. **Biomed Res. Int.**, v. 2015, ID 845340, 2015.

GOLL, M.G.; BESTOR, T.H. Eukaryotic cytosine methyltransferases. **Annu Rev Biochem**, v. 74, p. 481-514, 2005.

GOODENBERGER, M.L.; JENKINS, R.B. Genetics of adult glioma. Review. **Cancer Genet.**, v. 205, p. 613-621, 2012.

GROMMES, C. et al. Antineoplastic effects of peroxisome proliferator-activated receptor  $\lambda$  agonists. Review. **Lancet Oncol**, v.5, p. 419-429, 2004.

GROMMES, C. et al. Inverse association of PPAR gamma agonists use and high grade glioma development. **J. Neuro. Oncol.**, v.100, p. 233-239, 2010.

GROMMES, C. et al. “The PPAR $\gamma$  agonist pioglitazone crosses the blood-brain barrier and reduces tumor growth in a human xenograft model,” **Cancer Chemoth Pharm**, v. 71, n. 4, p. 929-936, 2013.

HAU, P. et al. “Low-dose chemotherapy in combination with COX-2 inhibitors and PPAR-gamma agonists in recurrent high-grade gliomas-a phase II study,” **Oncology**, v. 73, n. 1-2, p. 21-25, 2007.

<http://portal.anvisa.gov.br>

JENKINS, R. B. et al. A t(1;19)(q10;p10) mediates the combined deletions of 1p and 19q and predicts a better prognosis of patients with oligodendrogloma. **Cancer Res.**, v.66, n.20, p.9852-9861, 2006.

JIAPAER, S. et al. Potential Strategies Overcoming the Temozolomide Resistance for Glioblastoma. Review Article. **Neurol Med Chir**, v. 21, p.1-17, 2018.

LEE, M.W. et al. Cell death is induced by ciglitazone, a peroxisome proliferator-activated receptor gamma (PPAR gamma) agonist, independently of PPAR gamma in human glioma cells. **Biochem. Bioph. Res. Co.**, v.417, p. 552-557, 2012.

LIU, L. and LI, X. IDH Gene Mutation in Glioma. Mini Review. **Cancer Transl Med**, v.4, n.5, p. 129-133, 2018.

LIU, X. et al. Discovery and SAR of thiazolidine-2,4-dione analogues as insulin-like growth factor-1 receptor (IGF-1R) inhibitors via hierarchical virtual screening. **J.Med.Chem.**, v. 53, p. 2661-2665, 2010.

MALTA, T.M. et al. Glioma CpG island methylator phenotype (G-CIMP): biological and clinical implications. **Neuro-Oncol.**, v. 20, n.5, p. 608-620, 2017.

METWALLY, K; PRATSINIS, H.; KLETSAS, D. Novel 2,4-thiazolidinediones: Synthesis, in vitro cytotoxic activity, and mechanistic investigation. **Eur. J. Med. Chem.**, v.133, p. 340-350, 2017.

MOROSETTI, R. et al. The PPAR gamma ligands PGJ2 and rosiglitazone show a differential ability to inhibit proliferation and to induce apoptosis and differentiation of human glioblastoma cell lines. **Int. J. Oncol.**, v. 25, p. 493-502, 2004.

MOVAHEDA, Z. G. et al. Cancer cells change their glucose metabolism to overcome increased ROS: One step from cancer cell to cancer stem cell? **Biomed & Pharmacother.**, v. 112, 108690, 2019.

MUGHAL, A. et al. Effects of Thiazolidinediones on metabolism and cancer: Relative influence of PPAR $\gamma$  and IGF-1 signaling. **Eur. J. Pharmacol.**, v.768, p. 217-225, 2015.

MUR, P. et al. Impact on prognosis of the regional distribution of MGMT methylation with respect to the CpG island methylator phenotype and age in glioma patients. **J Neuro Oncol.**, v.122, n.3, p.441-450, 2015.

NAPOLEON, A.A. Review on recent developments and biological activities of 2,4-thiazolidinediones. **Int. J. Pharm. Tech. Res.**, v.9, n.3, p.429- 443, 2016.

OSTROM, Q.T. et al. CBTRUS statistical report: primary brain and central nervous system tumors diagnosed in the united states in 2007–2011. **Neuro-Oncol.**, v.16, p.iv1–iv63, 2014.

OSTROM, Q.T. et al. The epidemiology of glioma in adults: a “state of the science”. Review. **Neuro-Oncol.**, v.16, p. 896-913, 2014.

OSTROM, Q.T. et al. CBTRUS Statistical Report: Primary Brain and Other Central Nervous System Tumors Diagnosed in the United States in 2012–2016. **Neuro-Oncol.**, v.21, n.5, 2019 (ISSN: 1523-5866)

PESTEREVA, E. et al. PPAR $\gamma$  agonists regulate the expression of stemness and differentiation genes in brain tumour stem cells. **Br. J. Cancer**, v.106, n.10, p.1702-1712, 2012.

PLATE, K.H. et al. Vascular endothelial growth factor and glioma angiogenesis: coordinate induction of VEGF receptors, distribution of VEGF protein and possible in vivo regulatory mechanisms. **Int J Cancer**, v. 59, p. 520-529, 1994.

RADI, M. et al. Practical *one-pot* two-step protocol for the microwave-assisted synthesis of highly functionalized rhodanine derivatives. **Comb. Chem.**, v. 12, p. 200-205, 2010.

RÊGO, M.J.B.M. et al. Synthesis, in vitro anticancer activity and in silico study of new disubstituted thiazolidinedione derivatives. **Med. Chem. Res.**, v. 23, p. 3220-3226, 2014.

RHUN, E. L. et al. Molecular targeted therapy of glioblastoma. **Cancer Treat. Rev.**, v. 80, ID 101896, 2019.

SAMUDRA, N. et al. Seizures in glioma patients: An overview of incidence, etiology, and therapies. Review Article. J. Neurol. Sci., v. 404, p. 80-85, 2019.

SILVA, D.S. et al. Thiazolidin-4-ones from 4-(methylthio)benzaldehyde and 4-(methylsulfonyl)benzaldehyde: Synthesis, anti-glioma activity and cytotoxicity. **Eur. J. Med. Chem.**, v.124, p.574-582, 2016.

SILVEIRA, E.F. et al .Synthetic 2-aryl-3-((piperidin-1-yl)ethyl)thiazolidin-4-ones exhibit selective in vitro antitumoral activity and inhibit cancer cell growth in a preclinical model of glioblastoma multiforme. **Chem-Biol Interact**, v.266, p. 1-9, 2017.

STUPP, R. et al. Radiotherapy plus concomitant and adjuvant temozolomide for glioblastoma. **N. Engl. J. Med.**, v. 352, p. 987- 996, 2005.

SZABO, E. et al. Autocrine VEGFR1 and VEGFR2 signaling promotes survival in human glioblastoma models *in vitro* and *in vivo*. **Neuro-Oncol.**, v.18, p.1242–1252, 2016.

WAN, Z. et al. Peroxisome proliferator-activated receptor gamma agonist pioglitazone inhibits beta-catenin-mediated glioma cell growth and invasion. **Mol. Cell. Biochem.**, v. 349, p.1-10, 2011.

WEISENBERGER, D.J. Characterizing DNA methylation alterations from The Cancer Genome Atlas. Review series. **J. Clin. Invest.**, v.124, n.1, p.17-23, 2014

WELLER, M. et al. Glioma. **Nat. Rev. Dis. Primers**, v.1, ID 15017, 2015.

WU, H.; ZHANG Y. Mechanisms and functions of Tet protein-mediated 5-methylcytosine oxidation. **Genes Dev.**, v. 25, n. 23, p. 2436–2452, 2011.

WU, K. et al. Activation of PPAR $\gamma$  suppresses proliferation and induces apoptosis of esophageal cancer cells by inhibiting TLR4-dependent MAPK pathway. **Oncotarget**, v.7, n. 28, p. 44572-44582, 2016.

YE, Z.C.; SONTHEIMER, H. Glioma cells release excitotoxic concentrations of glutamate. **Cancer Res.**, v. 59, p.4383-4391, 1999.

YOUSEFNIA, S. et al. The influence of peroxisome proliferator-activated receptor  $\gamma$  (PPAR $\gamma$ ) ligands on cancer cell tumorigenicity. Review. **Gene**, v. 649, p. 14-22, 2018.

ZANDER, T. et al. Induction of apoptosis in human and rat glioma by agonists of the nuclear receptor PPAR $\gamma$ . **J Neurochem**, v.81,p. 1052-1060, 2002.

ZHAO, S., et al. Glioma-derived mutations in IDH1 dominantly inhibit IDH1 catalytic activity and induce HIF-1 $\alpha$ . **Science**, v. 324, n. 5924, p. 261-265, 2009.

## 7. ANEXOS

### 7.1 ANEXO A - COMITÊ DE ÉTICA EM EXPERIMENTAÇÃO ANIMAL DO ARTIGO E DO MANUSCRITO (CEEA 9219)



Pelotas, 10 de fevereiro de 2014

De: Prof. Dr. Éverton Fagonde da Silva

*Presidente da Comissão de Ética em Experimentação Animal (CEEA)*

Para: Professora Elizandra Braganhol

*Centro de Ciências Químicas, Farmacêuticas e de Alimentos*

Senhora Professora:

A CEEA analisou o projeto intitulado: "Investigação do potencial terapêutico de tiazolidinonas sintéticas para o tratamento de gliomas", processo nº 23110.009219/2013-55, sendo de parecer FAVORÁVEL a sua execução, considerando ser o assunto pertinente e a metodologia compatível com os princípios éticos em experimentação animal e com os objetivos propostos.

Solicitamos, após tomar ciência do parecer, reenviar o processo à CEEA.

Salientamos também a necessidade deste projeto ser cadastrado junto ao Departamento de Pesquisa e Iniciação Científica para posterior registro no COCEPE (código para cadastro nº CEEA 9219).

Sendo o que tínhamos para o momento, subscrivemo-nos.

Atenciosamente,

Prof. Dr. Éverton Fagonde da Silva

*Presidente da CEEA*

Ciente em: 02 / 04 /2014

Assinatura da Professora Responsável:

## 7.2 ANEXO B - COMPROVANTE DE PUBLICAÇÃO NA REVISTA MEDICINAL CHEMISTRY

07/05/2020 2,4-Thiazolidinedione as Precursor to the Synthesis of Compounds with Antiglioma Activities in C6 and GL261 Cells | Bentham Sci...

The screenshot shows the Bentham Science website interface. At the top, there is a search bar with the placeholder "Search for..." and a search button labeled "Search". Below the search bar, there is a "Search in:" dropdown menu with options: All, Article, Chapter, and Book. A banner at the top of the page reads "NEW IN 2020 CORONAVIRUSES" and "JOIN EDITORIAL BOARD". The main content area displays the following information:

**Research Article**

**2,4-Thiazolidinedione as Precursor to the Synthesis of Compounds with Antiglioma Activities in C6 and GL261 Cells**

(E-pub Ahead of Print)

**Author(s):** Alana de Vasconcelos, Ana Júlia Zulian Boeira, Bruna Bento Drawanz, Nathalia Stark Pedra, Natália Pontes Bona, Francieli Moro Stefanello Wilson Cupido\*

[ORCID](http://orcid.org/0000-0003-2577-5323)

**Journal Name:** Medicinal Chemistry

**DOI :** 10.2174/1573406416666200403075826 (<https://doi.org/10.2174/1573406416666200403075826>)

[Journal Home \(node/627\)](#)

The screenshot shows the Eurekaselect website with a yellow header bar. The header bar contains the text "Become an Editorial Board Member" and a "Register Here" button.

(<http://www.eurekaselect.com/node/627/medicinal-chemistry/become-ebm-form/eabm>)

## 7.3 ANEXO C - COMPROVANTE DE SUBMISSÃO DO MANUSCRITO NA REVISTA ARCHIVES OF PHYSIOLOGY AND BIOCHEMISTRY

14/05/2020

Email – alana.vasconcelos – Outlook

### Archives Of Physiology And Biochemistry - Account Created in ScholarOne Manuscripts

Archives Of Physiology And Biochemistry <onbehalfof@manuscriptcentral.com>

Qui, 14/05/2020 11:07

Para: alanabdv@hotmail.com <alanabdv@hotmail.com>

14-May-2020

Dear Miss Alana Vasconcelos:

A manuscript titled 3-(4-fluorobenzyl)-5-(4-methoxybenzylidene)thiazolidine-2,4-dione exhibits antglioma effect and reverts behavioral and biochemical changes in an experimental model of glioma (NAPB-2020-0396) has been submitted by Miss Alana Vasconcelos to Archives Of Physiology And Biochemistry.

You are listed as a co-author for this manuscript. The online peer-review system, ScholarOne Manuscripts, has automatically created a user account for you.

The site URL and your USER ID for your account is as follows:

SITE URL: <https://mc.manuscriptcentral.com/napb>

USER ID: alanabdv@hotmail.com

[https://mc.manuscriptcentral.com/napb?URL\\_MASK=8e3b881642cf486f8a4d5da19a4c9c07](https://mc.manuscriptcentral.com/napb?URL_MASK=8e3b881642cf486f8a4d5da19a4c9c07)

Please note that your password is case-sensitive.

When logged into the site you will be able to check the status of papers you have authored/co-authored. Please do log in to <https://mc.manuscriptcentral.com/napb> to update your account information, and to change your password to one of your choice.

Thank you for your participation.

Sincerely,

Archives Of Physiology And Biochemistry Editorial Office

Log in to Remove This Account - [https://mc.manuscriptcentral.com/napb?URL\\_MASK=1ea5e3efa4fd485da9862e4b7fc16ea2](https://mc.manuscriptcentral.com/napb?URL_MASK=1ea5e3efa4fd485da9862e4b7fc16ea2)